Stony Brook University

The Interplay Between Adenovirus and the Double-Strand Break Repair Response in the Struggle to Replicate

A Dissertation Presented

by

Kasey Anne Karen

to

The Graduate School

in Partial Fulfillment of the

Requirements

for the Degree of

Doctor of Philosophy

in

Molecular Genetics and Microbiology

Stony Brook University

August 2009

Stony Brook University

The Graduate School

Kasey Anne Karen

We, the dissertation committee for the above candidate for the

Doctor of Philosophy degree, hereby recommend

acceptance of this dissertation.

Dr. Patrick Hearing, Ph.D – Advisor
Professor, Molecular Genetics and Microbiology

Dr. Carol Carter, Ph.D – Chairperson of Defense
Professor, Molecular Genetics and Microbiology

Dr. James Bliska, Ph.D
Professor, Molecular Genetics and Microbiology

Dr. David L. Spector, Ph.D
Professor, Cold Spring Harbor Laboratory

This dissertation is accepted by the Graduate School

Lawrence Martin
Dean of the Graduate School

Abstract of the Dissertation

The Interplay Between Adenovirus and the Double-Strand Break Repair Response in the Struggle to Replicate

by

Kasey Anne Karen

Doctor of Philosophy

in

Molecular Genetics and Microbiology

Stony Brook University

2009

The Adenovirus genome is structured as a linear double-stranded DNA molecule covalently linked to terminal protein at each end and at times during an infection and within the virion, coated by viral protein VII. The double-strand break repair proteins can perceive this DNA structure as a double-strand break and elicit a checkpoint signaling response and DNA repair program that results in genome concatenation unless the DSBR response is inactivated in some way. The viral proteins, E4 ORF6 and E1B 55K, form an E3 ubiquitin ligase complex with other cellular proteins to cause the specific degradation of several known cellular substrates. One of these substrates is the Mre11 protein of the MRN complex, which is the sensor of DSBs. Inactivation of this complex is necessary for efficient viral DNA replication and a productive infection to occur. I have shown that E4-ORF6/E1B-55K-dependent degradation of Mre11 occurs prior to the onset of viral DNA accumulation. A functional assay was also performed to show that the DSBR response is inhibited to such a degree during infection that a checkpoint signaling response is not elicited even after newly-introduced

DSBs are formed from ionizing radiation. TP was also found still attached to mutant genomes that are unable to inhibit the MRN complex at a time when checkpoint signaling was induced. This suggests that TP is not the protective factor that prevents checkpoint signaling during the immediate early phase of viral infection from the DSBR response. It also suggests that degradation of the termini of the genome, which contains the origins of replication, and which would cleave TP off, is not an important factor for the viral DNA replication block. Finally, it is also shown that viral protein VII may serve as the protective factor early during infection and that with higher levels of transcription, causing the release of VII, the MRN complex can recognize the DNA ends and elicit a checkpoint signaling response. It is also proposed that the formation of these complexes on the genomes can prevent the formation of pre-initiation complexes required for viral DNA replication.

Table of Contents

List of Abbreviations

Ad	adenovirus
CAR	coxsackie-adenovirus receptor
TP	terminal protein
kb	kilobase
bp	base pair
ITR	inverted terminal repeat
ORF	open reading frame
MRN	Mre11-Rad50-Nbs1
POD	PML oncogenic domain
ND10	nuclear domain 10
HSV-1	herpes simplex virus type 1
HCMV	human cytomegalovirus
hpi	hours post-infection
MTOC	microtubule organizing center
DSBR	double-strand break repair
DSB	double-strand break
ATM	ataxia-telangiectasia
ATR	ATM-Rad3-related
NHEJ	non-homologous end joining
Mdc1	mediator of DNA damage checkpoint 1
NLS	nuclear localization signal
FHA	forkhead-associated
BRCT	BRCA1 C-terminus
AFM	atomic force microscopy
IR	ionizing radiation
HAT	histone acetyltransferase
pATM	phosphoATM
UV	ultraviolet
HU	hydroxyurea

MMS	methyl methanesulfonate
PIKK	phosphotidyl inositol 3-kinase-like kinase
RPA	replication protein A
ATRIP	ATR-interacting protein
IRIF	ionizing radiation-induced foci
CK2	casein kinase 2
A-T	ataxia-teangiectasia
ATLD	A-T-like disorder
NBS	Nijmegen breakage syndrome
RDS	radiation-resistant DNA synthesis
PAMPs	pathogen-associated molecular patterns
TLR	Toll-like receptor
LPS	lipopolysaccharide
ER	endoplasmic reticulum
IFN	interferon
pTP	pre-terminal protein
dCMP	deoxycytidine monophosphate
TAF-I	template-activating factor I
AraC	cytosine arabinose
ChIP	chromatin immunoprecipitation
qPCR	quantitative PCR
FITC	fluorescein isothiocyanate
TRITC	tetramethyl rhodamine isothiocyanate
ChIP–reChIP	sequential ChIP
Ad pol	adenovirus polymerase

List of Figures

Acknowledgements

I would first like to thank my thesis advisor, Dr. Patrick Hearing, for always being there for me throughout these last six years as I worked towards completing my dissertation. He has been an incredible mentor and role model. I will always aspire to be as hard-working, kind, and patient as he has proven to be, but it seems like quite a daunting task. We, in the lab, have a running joke that we need to get GPS on Pat since he's always moving from his office, to the lab, to a meeting, but he would always make time when asked and never let anyone stray too far. The things I've learned from working with him will be with me always. Knowing that he genuinely cares for me and has my best interests at heart gives me the confidence to move on and pursue an academic career because I know that he will always be in my corner.

I would also like to thank the rest of the lab, past (Amanda, Mark, Mary, Matt, Indy, Vanessa, Sharanya, Jared and Jihong) and present (Mena, Janet, Liz, Kai, Ilana, Hsin-Chieh, Suk-Young, and Ting). I truly feel like I've been spoiled here and will never find another lab that is as friendly, fun, productive, supportive, and caring as our lab. It was exactly the kind of environment that I thrive in. Even when my experiments weren't looking very promising, knowing that I would get to spend the day with my labmates would cheer me up. It was always a pleasure to come to lab and there has always been delicious food waiting for me there.

I also have to give myself a pat on the back for choosing to ask Dr. Carol Carter, Dr. James Bliska, and Dr. David Spector to be a part of my thesis committee and to thank them for accepting. I would also like to thank Dr. Dafna Bar-Sagi for being part of my thesis proposal committee. Each committee meeting was filled with good questions and suggestions in the most supportive way and I appreciate that more than I can say.

I would also like to thank Dr. David Ornelles for providing the dl1520/dl341 double mutant virus that was used in many of the experiments within this dissertation. Also, Dr. Arnold Berk provided the NTD-CUL5

construct that allowed us to do the elegant experiment involving the dominant negative Cullin5 mutant. Another key contribution to the experiments in the last half of my dissertation was the αVII antibody that was generously given to us by Dr. Dan Engel.

The Molecular Genetics & Microbiology Department has been a wonderful place to obtain a Ph.D. The faculty, staff, and students within have made a really warm community for us all to be a part of. Also, we work closely with the Genetics and Molecular and Cellular Biology programs, and between all three programs there exists a large network of friends that have proven to be a critical part of my graduate school career. Within this group of friends, I would like to give special thanks to Amanda, who was not only a labmate, but a very close friend throughout our entire graduate school careers and will continue to be for the rest of our lives. Also, Erin has been a true friend and helps to keep me sane by encouraging the ridiculousness that we do so well together. I'd also like to thank Beth, Lindsay, and Kate for being part of a very special group with Erin and myself known as The Royal Flush. And thank you to Gisselle, Kim, Betty, Nidia, and Teresa, the rest of my fellow micro class.

And finally, I need to thank my family. Coming to Stony Brook for graduate school meant coming back home since I grew up in the neighboring town, Setauket. My mom and dad have always been the most supportive people in my life and continuously encourage me to strive for more. And of course, I have to thank my sisters, Tara and Rebecca. Even though we are each very different, we share a bond that can never be broken. Having them by my side to vent to, or to help me get away from the lab, or to travel around Europe with has been such a comfort. I can always count on them for a good laugh—they never let me get too serious. I also want to thank my grandparents. My two grandmothers are such great women to look up to and my grandfather, who recently passed away, was one of the most unique and caring people I've ever known. I wish he could've seen me get my Ph.D. I know he would've been proud.

Introduction

Adenovirus Background

Adenoviruses have been studied since the 1950s when it was isolated from human adenoids and suspected to be the etiologic agent of acute respiratory disease found with many military recruits (122). Since then, many more serotypes have been discovered with 51 causing infections in humans. They belong to the family *Adenoviridae* and can be divided into two genera, *Mastadenovirus* and *Aviadenovirus*. *Mastadenovirus* species infect many different animals, including human, simian, bovine, and canine, whereas *Aviadenovirus* species are limited to birds. The human serotypes have been categorized into 6 subgroups (A-F) based on hemagglutination and cause a variety of diseases including, but not limited to, respiratory illness. Adenoviruses have been associated with epidemic conjunctivitis and gastrointestinal diseases as well. Usually, adenovirus causes localized, self-limiting infections, however, in immunocompromised patients, generalized infections may occur (122).

The focus of adenovirus studies has gone through several phases throughout the years. Early on, during the initial discovery years, human adenovirus (Ad) type 12 was shown to induce malignant tumors in newborn hamsters and began the search for viruses capable of oncogenesis (144). While tumorigenesis was seen *in vivo* here and a few Ad proteins were found to be sufficient to transform human cells in tissue culture (53), there is no epidemiologic evidence to suggest that Ad causes tumor formation in humans. Ad studies next turned to the discovery of mRNA splicing (10) and finally, focus had been turned to the virus' use as a gene therapy vector (43). Other aspects of study have also been done exploring the virus life cycle and interactions with various cellular processes.

All species of the *Adenoviridae* are non-enveloped with an icosahedral capsid ranging from 70-100 nm in diameter. The Ad genome is linear and composed of double-stranded DNA (122). During an infection, the virion will bind with high affinity to the coxsackie-adenovirus receptor (CAR), followed

by binding to αvβ3 or αvβ5 integrins, which causes structural changes that release fiber protein. The clustering of integrins induces clathrin-coated pit formation and endocytosis ensues (98, 99). Upon acidification of the endosome, penton undergoes conformational changes that expose hydrophobic regions and allows for the release of the virus into the cytoplasm (98). It then travels along microtubules to the nucleus and docks at a nuclear pore complex (19). The viral genome along with three viral proteins, terminal protein (17), VII, and mu, are translocated into the nucleoplasm (2, 17, 59, 92, 110, 114, 119, 151). Transcription of the immediate early gene, E1A, occurs, the mRNA is translocated to the cytoplasm, the protein is then translated and enters the nucleus, where it activates transcription of early region mRNAs, and regulates transcription of some cellular genes as well. The early region genes encode the proteins involved in viral DNA replication and in making the cellular environment more conducive to virus growth. Next, viral DNA replication occurs, along with transcription of late region mRNAs. Virions are then assembled, the cell is lysed, and the virions are released (43).

One of the most well-studied serotypes is Ad5 of the Group C subfamily, whose genome is just under 36 kilobases (kb) in length. At each end of the linear genome, there are inverted terminal repeats (ITRs) that extend for ~100 base pairs (bp) in length and contain the origins of replication (43, 54, 122). Adenovirus genes are divided into the immediate early gene, E1A, which only requires cellular proteins for its transcription, four early region transcription units (E1B, E2, E3, and E4), delayed early units (IX and IVa2), and the major late transcription unit that leads to five mRNAs (L1-L5). Transcription occurs on either strand depending on the transcription unit with transcription occurring in the rightward direction for E1A, E1B, E3, IX, and the major late units and the leftward direction for E2, E4, and IVa2. Early region genes are involved in regulating cellular processes to create an environment more amenable to virus growth, such as induction of the cell cycle and inhibition of apoptosis, the immune response to infection, and DNA repair mechanisms induced by viral DNA. Ad early genes also encode the viral

proteins necessary for DNA replication. The late region genes encode structural proteins and proteins involved in assembly and maturation (43, 122).

Adenovirus Early Region 4

The E4 region was shown to be important for viral DNA replication in that a deletion of the entire region showed normal early gene expression, but there was a viral DNA replication block. Infection with the E4-deleted virus also led to multimerization of genomes, known as concatemer formation, a decrease in late gene expression, and a severe defect in virus growth with the mutant being reduced 10^5 to 10^6 in virus yield as compared to wild type virus (54, 60, 152, 153). The E4 region contains six open reading frames (ORFs), 1-4, 6, and 6/7. Deletion of either ORFs 1-4 or ORF6 and 6/7 alone has little effect on virus growth as these mutants grow to near wild type levels in tissue culture, however, the deletion of both E4-ORF3 and E4-ORF6 results in a 1,000-fold loss in virus yield (44, 60). Either the E4-ORF3 or E4-ORF6 protein is individually sufficient to complement the DNA replication defect and virus growth (16, 60), thus these proteins are considered functionally redundant. One of the redundant functions is the inhibition of the Mre11-Rad50-Nbs1 (MRN) complex, however, the mechanisms of inhibition are vastly different (84, 154).

The E4-ORF3 protein functions by reorganizing cellular PML nuclear bodies into track structures (44, 133, 134). Studies have shown that E4-ORF3 is both necessary and sufficient for the reorganization to occur (133). PML nuclear bodies, also known as PML oncogenic domains (PODs), or nuclear domain 10 (ND10s), are nuclear matrix-associated punctate structures composed of a network of many different proteins, including Sp100, CBP, Daxx, p53, and SUMO-1 (6, 95, 96). A small subset of the total cellular population of the MRN complex is also present at PML nuclear bodies, although most of the MRN complex is found diffuse throughout the nucleus (34). There is a broad range of functions for the proteins found at PML bodies that include transcriptional regulation, DNA repair, apoptosis, and

protein modification (14, 167). The function of the nuclear body itself, however, is unknown. Some reports suggest active roles in cellular processes, such as transcription, RNA processing, and mRNA transport (14, 167). A direct role in transcription does not seem likely since no DNA or RNA are found within the nuclear bodies and the nuclear bodies are not found associated with sites of active transcription (13, 14). There is a tendency for PODs to be located near RNA processing compartments, such as Cajal bodies, cleavage bodies, and Sc35 domains and a connection to post-transcriptional regulation due to transport of mRNAs has also been made through direct interaction of PML with eIF4E in the nucleus (14). Also, an association of the POD with an antiviral response has been made since PML bodies increase in size and number when induced with interferon (95). Other reports suggest that PML bodies act as nuclear dumps or depots where proteins can be sent prior to degradation or temporarily to titrate the nucleoplasmic concentration (103).

DNA viruses often encode proteins that target ND10s for disruption. Herpes simplex virus type 1 (HSV-1) encodes the protein ICP0, which is an E3 ubiquitin ligase that targets PML and Sp100 for degradation and leads to the dispersal of ND10s (46). Human cytomegalovirus (HCMV) encodes the protein, IE1, which is necessary and sufficient to cause ND10 elimination (62). The Ad E4-ORF3 protein disrupts these nuclear domains by reorganizing them in a manner that has been found to disrupt the interferon response of infected cells (147). This is one aspect of PML disruption that is conserved over all Ad serotypes. Only in group C Ad serotypes, like Ad5, does the rearrangement of the PML bodies include the rearrangement of the MRN complex. It is also important to note that it is only group C Ad serotypes that can complement E4 mutant viruses for concatemer abrogation and late gene expression in tissue culture (134). The rearrangement of PML nuclear bodies into tracks by Ad5 E4-ORF3 involves relocalizing the MRN complex from a diffuse localization throughout the nucleoplasm to complete colocalization with PML and E4-ORF3 in the track structures. These tracks

can be seen by 6 hours post-infection (hpi) and results in a decrease in Mre11 solubility (4, 45). During a productive infection, when replication domains are established, the tracks surround these domains, but do not colocalize with them (45, 134). In this way, it is presumed that E4-ORF3 acts to sequester the MRN complex in the tracks away from the viral genomes and inhibit MRN activity.

Alternatively, E4-ORF6 carries out its function in inhibiting the MRN complex by usurping an E3 ubiquitin ligase complex with another viral protein, E1B-55K (55, 111). The viral component replaces the substrate-specificity proteins of the E3 ligase complex that includes the cellular proteins, elongins B and C, Cullin 5, and the RING protein, Rbx1 (166). In the normal cellular context, these proteins have been found to interact with Muf1, elongin A, WSB, and SOCS1, which are the presumed substrate-specificity factors (68). The complex needs to interact with an E2-conjugating enzyme that can conjugate ubiquitin chains to the specified target. This chimeric complex targets specific cellular proteins for proteasome-dependent degradation, such as p53, Mre11, DNA ligase IV, and integrin α3 (7, 36, 55, 111).

The cellular components have been shown to interact with E4-ORF6 alone, but E1B-55K requires E4-ORF6 to interact with elongins B and C, Cullin 5, and Rbx1 (55). Also, E1B-55K can pull down E4-ORF6, and each of the known targets of degradation, suggesting that E1B-55K specifies the substrates in this complex. When either E4-ORF6 or E1B-55K is deleted in a mutant virus, the degradation of these proteins is not seen following infection, showing their necessity (20, 112, 131, 133). Alternatively, when both of these proteins are expressed in a cell, they are sufficient to induce degradation of the target proteins (20, 117, 133). Also, treatment with proteasome inhibitors, such as MG132, prevent degradation, suggesting the dependence of the proteasome in the degradation pathway (133). In the literature, the timing of degradation had only been visualized through Western blot analysis and appeared to be a later event than the inhibition of the MRN complex by E4-

ORF3. By 12 hpi, Mre11 protein levels appeared to be reduced in levels by about half and most had been degraded by 18 hpi (133, 134).

Another mechanism employed by the virus to inhibit the MRN complex is relocalization to the cytoplasm. Mre11 is transported to the cytoplasm where it eventually forms aggresomes that are thought to increase the efficiency of proteasomal-dependent degradation and can inhibit DNA damage foci formation (4, 87). These aggresomes are not seen until late times during infection, however, proteins will generally aggregate in the cytoplasm and then move along microtubules to the MTOC (microtubule organizing center) to form an aggresome (49).

Double-Strand Break Repair

The inhibition of the MRN complex by Ad is important because it is involved in double-strand break repair (DSBR) and is regarded as the sensor of double-strand breaks (DSBs) (24, 34, 148). MRN becomes relevant to Ad infection because the linear, dsDNA genome can be perceived as DSBs upon translocation into the nucleus, which results in ligation of the genomes together forming large concatemers. To give a brief overview of the DSBR process, when a DSB occurs in the cellular genome due to a multitude of causes, ranging from ionizing radiation (93) to V(D)J recombination (30), the MRN complex recognizes the lesion and recruits the protein kinases, ataxia-telangiectasia mutated (ATM) and ATM-Rad3-related (ATR), to the site of the break to initiate the process of non-homologous end joining (NHEJ) (148). NHEJ involves resection of the DNA at the DSB to find regions of microhomology that can then be ligated together. The processing of the DNA generally results in small deletions within the DNA of around 1-5 nucleotides (nt).

The MRN complex may also initiate homologous recombination (HR) (127) to preserve the DNA sequence, however, in mammalian cells, this is thought to occur more during S phase when there is a sister chromatid available as a homologous template (86, 118, 129, 139). One study suggests that HR can begin to occur throughout interphase and that the proteins

involved in HR, which are different from those involved in NHEJ, are recruited to sites of DNA damage at a later time, while NHEJ proteins are the first to arrive (71). HR involves processing the DNA at the site of the lesion to yield 3' single-stranded ends that can then invade the double-stranded homologous template and prime synthesis to restore the genetic sequence disrupted at the DSB.

The two kinases, ATM and ATR, are central players in activating the cellular DNA damage response (42). Through intermolecular autophosphorylation, ATM is phosphorylated on S1981, resulting in the dissociation of dimers into monomers and enzymatic activation (8). ATM subsequently phosphorylates downstream effectors involved in checkpoint signaling, such as Nbs1 (50, 85) and H2AX (18, 116), and recruits other proteins involved in repairing the lesion. Large foci form at the site of the DNA break due to the accumulation of γH2AX, the phosphorylated form of the histone variant H2AX. γH2AX recruits, among other proteins, Mdc1 (mediator of DNA damage checkpoint 1) which serves as a bridge to sustain protein-protein interactions at the DNA lesion (136). DNA-PK along with DNA ligase IV/XRCC4 are involved in ligating the DNA ends together to repair the DSB (7).

Mre11 alone has both single-stranded endonuclease and 3'-5' exonuclease activity *in vitro*, however, that activity is stimulated in the presence of Rad50. As part of the MRN complex, Mre11 also has strand dissociation activity and can partially unwind DNA duplexes as well as the ability to mediate strand annealing between complementary ssDNA ends (37, 106). Mre11 can thus process the ends of the DNA lesion to yield regions of micro-homology between 1-5 nucleotides in length (105, 107, 145). The nuclease activity is directed by the Mn^{2+}-dependent calcineurin-like phosphoesterase motifs in the N-terminus of Mre11 and is separable from Mre11 binding to Rad50, Nbs1, and DNA (5, 48). Nuclease activity is stimulated in the presence of heterologous competitor DNA, however, if the DNA contains complementary sequences, degradation will be stimulated only

to the point where the complementarity begins (105). In this way, Mre11 is able to control the extent of degradation of the DNA ends and keep loss of genomic sequences to a minimum.

Rad50 is proposed to be involved in holding the two ends of DNA together by dimerizing through the coiled-coil domains (102). The central region is composed of two heptad repeats that fold anti-parallel to each other to form the coiled coil region. There are Walker A and B nucleotide-binding motifs at the amino- and carboxy-terminal domains that are brought together to form a globular domain by the protein folding back on itself. The globular domain of Rad50 has ATPase and adenylate kinase activity, which is important for regulating DNA binding and Mre11 nuclease activity (12, 38, 58). Bhaskara *et al*. propose that there may be three separable Rad50 functions that require different nucleotide-bound states (12). Nonhydrolyzable ATP analogs stimulate DNA binding by Mre11/Rad50 complexes, suggesting that ATP binding alone is sufficient for this function. On the other hand, for the MRN complex to partially unwind DNA duplexes, ATP hydrolysis is required. And finally, DNA tethering is stimulated only when there is both ATP hydrolysis and adenylate kinase activity present in Rad50.

Mre11 and Rad50 form the core of the MRN complex and are found in a heterotetrameric assembly (M_2R_2) with distinct head, coil, and hook domain regions (102). Atomic force microscopy (AFM) studies reveal a conformational switch in the M_2R_2 structure upon DNA binding that allows for long-range tethering. Rad50 homodimerizes through the CXXC motif, found at the apex of the coiled coil domain, which can coordinate binding through the presence of a Zn^{2+} ion and form a Zn hook. The intramolecular Zn hook of M_2R_2 is formed between the flexible coiled coil domains of Rad50 and result in a circular structure with connections at the head domain and the hook domain and with the coil domains being bent outward. Upon, DNA binding, the coiled coil domains become more rigid and are found parallel to each other preventing a connection via the Zn hook. Long-range DNA tethering is thus made possible by allowing the free CXXC motifs to interact

with Rad50 molecules from a separate M_2R_2 complex bound to another piece of DNA. Similar experiments were also done with Nbs1 present and were found to have similar results with Nbs1 binding at the head domain. It was also determined that once loaded on the DNA, the MRN complex can slide along the DNA (102, 158).

Nbs1 is important in directing the localization of the MRN complex and propagating the checkpoint signaling response. In cells that lack Nbs1, which contains a nuclear localization signal (NLS), and an Mre11-binding domain, Mre11 and Rad50 remain cytoplasmic (39). Also, the forkhead-associated (FHA) and BRCA1 C-terminus (BRCT) domains of Nbs1 are located in the N-terminus and involved in binding directly to γH2AX and retaining the MRN complex at the site of the DNA lesion (40, 73). There is an ATM binding site in the C-terminal tail of Nbs1 that is important in the initial activation of ATM through autophosphorylation (25). There are also SQ motifs within the central region that are consensus sequences of phosphorylation by ATM or ATR. Serine residues 278 and 343 are phosphorylated by ATM in response to radiation and are associated with the checkpoint signaling that is elicited (85, 164). Three parallel pathways have a role in the intra-S cell cycle checkpoint. There are the two Nbs1-dependent pathways, ATM/NBS1/SMC1 and ATM/FANCD2, and the NBS1-independent pathway, ATM/CHK2/CDC25A/CDK2, which may be able to function at higher levels of DNA damage (73).

ATM is a protein kinase of the phosphotidyl inositol 3-kinase-like kinase (PIKK) family that acts both up- and downstream of the MRN complex. It exists as an inactive dimer that dissociates into an active monomeric state in response to DSBs. *In vitro* studies have shown that activation of dimeric ATM can occur when in the presence of both linear DNA of greater than 200bp and the MRN complex (78, 163). ATM activation is inhibited after irradiation in the presence of mutant Mre11 that is nuclease-defective, Mre11-3, suggesting that merely MRN recognition is insufficient for activation and that the nuclease activity of Mre11 is a requirement (148). Although, an *in*

vitro study showed that in conditions that do not allow Mre11 nuclease activity (without Mn^{2+}), ATM activity was retained (78). The ATP-dependent unwinding of the DNA did, however, seem to be necessary for ATM activation *in vitro* (78). Activation of ATM occurs by intermolecular autophosphorylation on at least three serines, S367, S1893, and S1981 (75).

phosphoATM (pATM) that has been activated by the presence of DNA and the MRN complex from a *Xenopus* egg extract, isolated from the DNA, and exposed to fresh extract without DNA, cannot cause the activation of ATM from the fresh extract. This suggests that the presence of DNA is still required (163). Other studies have shown the requirement of Tip60, a histone acetyltransferase (HAT) in the activation of ATM (137). The acetylation of ATM on lysine 3016 by Tip60 is required for activation of ATM kinase activity. There have also been studies with *Xenopus* egg extracts that suggest nucleosome structure or histone modifications may play a role in ATM activation, supported by the fact that 200bp, the minimum requirement for ATM activation, is also about the length required for the assembly of a single nucleosome (163). ATM may also have a role in repressing degradation of the ends of DSBs as seen by the deletion of ATM in cells resulting in the repair of DSBs with larger stretches of deletions (113).

ATR is a similar protein kinase of the PIKK family that has been shown to be able to compensate for ATM function in some ways. It appears to be activated primarily by ultraviolet (UV) radiation, hydroxyurea (HU), and methyl methanesulfonate (MMS). There is also evidence to suggest an ATM to ATR switch upon resection of the DNA ends to yield longer stretches of ssDNA that can be coated by the replication protein A (RPA), which can recruit ATRIP (ATR-interacting protein) and ATR. ATR elicits a checkpoint signaling response similar to ATM, however, several of the phosphorylation substrates are different, such as Chk1 (32, 65, 126, 169).

H2AX is a histone variant, making up about 10-15% of total H2A levels in higher organisms, and may be the first protein phosphorylated by ATM, other than itself, in response to DSBs (18, 23). It is phosphorylated on serine

139 creating γH2AX and is involved in promoting the sustained binding of many proteins to the sites of DSBs (116). Phosphorylated H2AX seems to initiate the formation of large ionizing radiation-induced foci (IRIF) by covering large flanking regions of the DSB. In mammalian cells, γH2AX is estimated to form on chromosomal regions megabases in length away from the DSB (115). In *Saccharomyces cerevisiae*, a single DSB of known sequence can be formed by creation of an HO endonuclease site. Determination of the protein content of the chromatin surrounding that break can be observed through ChIP analysis. In yeast, γH2AX is not found as far away from the break as in mammalian cells, however, it has been found up to 30 kb away with peak concentration around 3-5kb away (127). Interestingly, within 1kb of the break, γH2AX enrichment is not increased, while Mre11 is enriched (127). There is also an increase in the fraction of ATM that is resistant to detergent extraction observed following ionizing radiation (IR) that is thought to be due to IRIF formation (148). While MRN can bind to DNA as a first responder and does not require other proteins to be present for the initial recognition, the formation of sustained foci that include the MRN complex requires the binding of Nbs1 to γH2AX through its FHA/BRCT domain. In fact, γH2AX is not necessary for the initial recruitment of the MRN complex, BRCA1, or 53BP1 to DSBs, however, sustained retention of these proteins and recruitment of other IRIF proteins require both γH2AX and Mdc1 (22, 90, 132, 136).

Loss of Mdc1 reduces phosphorylation of H2AX and one model proposes that Mdc1 controls the dephosphorylation of γH2AX (135). Mdc1 itself is also phosphorylated on a cluster of conserved SDT repeats by casein kinase 2 (CK2) (27, 100, 130). This phosphorylation is constitutive and allows Mdc1 to directly interact with Nbs1, which can facilitate the sustained binding of the MRN complex at sites of DNA damage (51, 130, 132). As do many other proteins involved in DSBR, Mdc1 also contains both FHA and BRCT domains. The FHA domain is important in transducing the checkpoint signal elicited by DSBs in that the interaction with pChk2-T68 is inhibited when the FHA domain is deleted and there is a defective S-phase checkpoint and

decreased apoptosis seen with these mutants (89). It seems that Mdc1 also mediates the direct interaction between γH2AX and ATM, which increases the accumulation of activated ATM at the regions flanking the DSB, thus promoting a feedback loop that expands H2AX phosphorylation and can amplify the checkpoint signaling pathway (88).

Null mutations of some of the genes encoding proteins involved in DSBR are embryonic lethal in mice, such as with ATM and each component of the MRN complex (91, 160, 168). Patients with hypomorphic mutations in these genes have been observed and cells isolated from these patients have been cultured. Ataxia-telangiectasia (A-T) is the disease caused by biallelic mutations in the *ATM* gene. The major clinical features are progressive cerebellar ataxia and telangiectasia (dilated blood vessels, usually in the eyes), immunodeficiency, genomic instability, predisposition to lymphoreticular malignancies, and hypersensitivity to IR (142). Hypomorphic mutations in Mre11 lead to A-T-like disorder (ATLD) and patients present with very similar clinical characteristics as A-T patients, except there is no telangiectasia and the neurodegeneration is slower. Nijmegen breakage syndrome (NBS) patients have mutations in the *NBS1* gene and there has been one recorded case with mutations in *RAD50* that led to a disease indistinguishable from NBS. This syndrome is characterized by microcephaly, growth retardation, mental deficiency, immunodeficiency, radiation sensitivity, chromosomal instability, and cancer predisposition (41, 141, 148).

The cellular phenotype for all three is very similar and characterized by various degrees of radiosensitivity and impairment of the cellular response to DSBs. Radiation-resistant DNA synthesis (RDS) is seen and results from a defect in the intra-S cell cycle checkpoint so that the cell will continue to synthesize DNA in the presence of radiation-induced DNA damage (148). Genetically, there are two variants present in patients with ATLD. The moderate version, ATLD(M), has reduced levels of partially active Mre11 from heterozygous mutations resulting in one nonsense and one missense mutation. ATLD(S), the severe form, is the result of two nonsense mutations

leading to extremely low levels of truncated Mre11 protein. NBS patients have homozygous hypomorphic mutations in *NBS1* producing two truncated versions of Nbs1, one of which is found in the MRN complex and may have residual activity (148).

Adenovirus and Double-Strand Break Repair

Many studies have been done evaluating the importance of inhibiting the DSBR response during Ad infection to study the interplay between these two systems. By interrupting certain parts of the pathway in order to prevent recognition of its genome, Ad infection serves as an interesting way to understand what is necessary to elicit a response and how to prevent such a response from occurring. When infected with an E4-deleted virus (or one in which both E4-ORF6 and E4-ORF3 are mutated), there are several detrimental effects that are all related to the activity of the DSBR response. There is an inhibition of viral DNA replication, concatenation of the viral genomes, a checkpoint signaling response, a reduction in late protein synthesis, and ultimately, a severe defect in virus growth (16, 44, 54, 60, 64, 152, 153).

Different cell lines with mutations in different proteins involved in various parts of the DSBR pathway were used in Ad infections where E4-ORF6 and E4-ORF3 were mutated. The use of ATLD or NBS cells rescued mutant virus growth, while deletions in the genes for DNA ligase IV, BLM (Bloom helicase), or DNA-PK, did not affect the growth defect seen with such a mutant virus (45). This suggests that the MRN complex is necessary and sufficient to inhibit virus growth. The effect the MRN complex has on viral DNA replication has also been studied and shows that through RNA knockdown and the use of ATLD and NBS cells, rescue of viral DNA replication occurs in E4-deleted Ad infections (77, 94). There is also a mutant Nbs1 protein that can inhibit viral DNA replication, but is unable to bind ATM and does not elicit a checkpoint signaling response nor does it induce concatemer formation (77). These data uncouple the two phenotypes and

show that the defect in viral DNA replication is not due to concatenation as some had speculated.

Other evidence to suggest that viral DNA replication and concatenation are separable involves observing a viral DNA replication defect during E4 mutant infections in cells deficient in proteins necessary for concatenation, such as DNA-PK. The function of DNA-PK in Ad infection was studied to observe the role DSBR had in concatemer formation. MO59J cells, which lack DNA-PK, were infected with E4-deleted virus and found to prevent concatemer formation, while concatemers of up to at least seven genomes in length were formed in MO59K cells, which were isolated from the same human glioma, but express DNA-PK (15). In either cell line, MO59K or MO59J, whether concatenation occurs or not, viral DNA replication of E4-deleted viruses is significantly inhibited suggesting that concatenation does not contribute to the viral DNA replication block (94). These experiments were reiterated with a virus that lacks E1B-55K and E4-ORF3 and is similarly unable to inhibit the MRN complex (123). Also, in the opposite way, there are E4-ORF3 point mutants, which in the background of an E4-ORF6 mutant, allows for significant concatenation, while they did not interfere with viral DNA replication (44). Since concatenation is a late effect, it is possible that some E4-ORF3 mutants can inhibit the MRN complex enough to allow for viral DNA replication, but as the amount of viral genomes within the nucleus increases, it cannot contain the MRN complex completely and concatenation ensues.

More experiments have been done with MO59J cells in which it was discovered that concatenation does appear to affect late gene expression in infections with E4-deleted virus (64). In MO59J cells, which have a defect in viral DNA replication, but no genome concatenation, the late gene expression is rescued. Even though late mRNA levels are reduced during infection with E4-deleted virus, the rate of transcription remains the same as with wild type infection, suggesting that the E4 proteins may have a role in stabilizing late viral mRNAs (120).

Other Viruses and DSBR

Cellular innate immunity is the frontline of defense that responds to many different forms of pathogens by recognizing them as non-self entities by sensing pathogen-associated molecular patterns (PAMPs). Toll-like receptors (TLRs) are transmembrane receptors that detect extracellular PAMPs (70). Bacteria have many PAMPs that are recognized by the cell, such as lipopolysaccharide (LPS), peptidoglycans, lipoproteins, flagellin, and CpG DNA, however a virus is less complex and thus, less recognizable as different from the host (72). The TLRs involved in detecting viral nucleic acids are TLR3, TLR7, TLR8 and TLR9, and are localized to the endosome or endoplasmic reticulum (ER) rather than the cell surface (70). TLR3 recognizes dsRNA, TLR7 and TLR8 recognize ssRNA, and TLR9 recognizes unmethylated CpG motifs that are found in viruses like HSV-1 (70). All TLRs elicit downstream signaling events involving transcription factors such as, IRF3, IRF7, or NF-κB, to activate transcription of type I interferon (IFN) and inflammatory cytokines (70). RIG-I, Mda5, and LGP2 are alternative receptors that recognize dsRNA in the cytoplasm and similarly activate transcription of type I IFN and inflammatory cytokines (70). Another inducer of type I IFN and inflammatory cytokines is the cytoplasmic dsDNA sensor, DAI. DAI is known to respond to the DNA virus, HSV-1 (138), and Ad is presumed to be involved in activating the inflammasome through DAI (138).

The DSBR pathway is not only capable of recognizing structurally uncharacteristic cellular DNA, but also viral DNA that exists in a linear state during the life cycle of DNA viruses, as well as retroviruses. In this way, it can serve as an innate immune response of the host. During the evolution of these viruses, however, some have manipulated the DSBR machinery so that it plays a beneficial role in their life cycle. Ad is unique in that it is linear and clearly remains that way throughout infection. Other linear dsDNA viruses, such as herpesviruses, tend to circularize upon infection and remain that way in an episomal state during latency or will use theta replication and/or rolling circle replication during the lytic cycle (63, 97, 109). These forms of

replication yield circular or concatemeric genome products that are later cleaved during packaging. Adenovirus is thus unique in that the MRN complex and the DSBR machinery as a whole have a clear detrimental effect on virus replication. With other viruses, it appears more complicated in that they have evolved to utilize the DSBR pathway to their advantage and also have ways to inhibit it. For example, experiments have been done with deficient cell lines, RNAi knockdown, and specific chemical inhibitors to effect proteins involved in the DSBR pathway, that show that this pathway is beneficial for virus replication in the case of HSV-1 and SV-40 (83, 125). The HSV-1 IE protein, ICP0, degrades DNA-PKcs (104) and mislocalizes ATRIP (155), thereby inactivating the repair pathway. Also, SV-40 T antigen is a substrate for pATM (125), but can downregulate the MRN complex in a proteasome-dependent manner (165). It was also shown that the activation of ATM, was necessary for localization of T antigen to viral replication centers and the subsequent degradation of the MRN complex (165). It is a common theme for viral replication centers of DNA viruses to contain members of the DSBR pathway (21, 35, 143, 156).

The Incoming Genome

One of many unresolved issues is how the incoming viral genome evades detection by the MRN complex prior to production of the early genes that inhibit the complex. As mentioned previously, there are three viral proteins that enter the nucleus along with the genome during the initial stage of infection; TP, VII, and mu. Since the MRN complex is capable of recognizing a single DSB within the cell and causing an arrest at the G2/M checkpoint (80), the virus must have evolved a mechanism to mask its genome and it seems likely that it would be one of the proteins that is found associated with the genome within the virion and throughout the early phase of infection.

Not much is known about viral protein mu. It is a small protein of 19 amino acids in its mature form after the cleavage of the amino- and carboxy-termini of the 79 amino acid precursor (28). Mu can precipitate negatively-

charged DNA via the nine positively-charged arginine amino acids, which suggests that it plays a role in DNA condensation in the core of the virions (3).

TP is covalently linked to the 5' end of the viral genome and is involved in priming the viral DNA replication reaction. In order for replication to ensue, a pre-initiation complex must form at the origins of replication on the viral genome (122). Pre-terminal protein (pTP), the precursor protein of TP, is covalently linked to a deoxycytidine monophosphate (dCMP) molecule through a phosphodiester bond between the β-hydroxyl group of serine residue 580 of pTP and the 5'-hydroxyl of dCMP (26, 82, 128). It is thought that the nucleolytic activity of Mre11 may be involved in cleaving TP from the genome as it has a similar function in cleaving Spo11 off the *Saccharomyces cerevisiae* meiotic-specific DSBs (101). This led to the speculation that it is the cleavage of TP by Mre11 that allows for full recognition of the Ad termini as DSBs (133).

Viral protein VII is considered the major core protein as it is present at 1080 copies per genome and comprises 14% of the total weight of the virion (74). It is noncovalently bound to the viral DNA within the capsid and remains associated with the DNA throughout the early phase of infection, being released at around 10 hpi (29). VII is a highly basic protein with α-helical segments that suggest VII is a hybrid of histone and protamine proteins (1). The exact structure of VII bound to DNA within the nucleus is not known, however, micrococcal nuclease digestion has shown that it does appear to form nucleosome-like structures (121, 140). Also, electron micrographs of the viral chromatin do show a regular pattern resembling beads on a string (150).

In vitro studies have shown that VII has an inhibitory effect on viral transcription and DNA replication (66, 74, 81, 149). VII and E1A have been found to associate both *in vitro* and *in vivo*, leading to relief of transcriptional repression (66, 161). This association may result in remodeling of the Ad DNA/protein VII complex, which is critical for efficient transcription and replication. The host protein, template-activating factor I (TAF-I), was determined to be a stimulator of Ad transcription *in vitro* (56). TAF-I both

interacted with VII in an immunoprecipitation assay and colocalized with VII in immunofluorescence assays performed during the early phase of infection. Also, knockdown of TAF-I delayed early transcription in an Ad infection (56). TAF-I is suggested to have a role in remodeling cellular chromatin and it is thought to effect viral chromatin in a similar way.

Transcription also has an important role in remodeling viral chromatin in that it is responsible for the release of VII from the DNA (29). Immunofluorescence and chromatin immunoprecipitation (ChIP) assays show that VII remains on the viral genomes until about 10 hpi (29, 161). Studies were done with the transcriptional inhibitor, α-amanitin, the DNA replication inhibitor, cytosine arabinoside (araC), and the E1A-deleted Ad virus, dl312, to determine that the release of VII is due to transcription and not replication. Gutted vectors with the Ad packaging domain and ITRs flanking 28 kb of human non-coding sequences, or non-coding sequences with GFP under the control of the CMV promoter, were also used to show that transcription itself is sufficient to release VII from viral DNA (29). It is thought that the release of VII is caused by the elongation RNA polymerase passing through the DNA or transcription-associated chromatin remodeling complexes.

Significance and Specific Aims

The connection between Ad and the DSBR pathway allows for the study of Ad proteins and the viral life cycle as well as the proteins involved in DSBR, particularly the MRN complex. The ability to easily manipulate the viral genome and create different conditions within the cell is very advantageous toward dissecting different parts of the DSBR pathway and determining the necessary features of the Ad virus in terms of efficient viral DNA replication or preventing viral DNA concatenation. DSBR is a well-studied cellular process due to the substantial stress that DSBs cause on a cell and its implications with cancer when disregulated.

The results of my dissertation suggest a model in which the Ad genome evades detection by the MRN complex by VII-binding and that VII release does not occur until after E4-ORF6/E1B-55K have degraded Mre11, thus preventing competition between pre-initiation complex formation and MRN binding which would lead to a significant decrease in viral DNA replication. Specifically, I have extrapolated this information by seeking to answer the following:

1. Confirm that the Ad early proteins, E4-ORF6 and E1B-55K, are capable of inhibiting the MRN complex by proteasome-dependent degradation prior to the onset of viral DNA replication. Since a block at the level of viral DNA replication is an important phenotype of cells infected with a virus that is unable to inhibit the MRN complex, this inhibition should occur before replication begins, but the degradation had not been shown to occur by such a time point in the literature.
2. Determine whether TP cleavage occurs on viral genomes at a time when viral DNA replication was ongoing. The answer to this inquiry would lead to insights into the mechanism of viral DNA replication inhibition during infections with mutant viruses that are unable to inhibit the MRN complex. One hypothesis is that the nuclease activity of Mre11 plays a role by degrading the termini of the viral genomes, which contain the origins of replication. Terminal degradation would also result in TP cleavage.

3. Explore the initial recognition of the viral genome as a DSB and how it is delayed for several hours after translocation into the nucleus. Focus on viral protein VII has led to a novel model that describes the mechanism of MRN evasion as well as discusses a possible explanation for the mechanism of inhibition of viral DNA replication. Several mechanisms had been hypothesized, but most have been discredited due to new research. The proposed model explores a novel mechanism of inhibition of viral DNA replication that involves competition between the viral DNA replication machinery and the DSBR pathway.

Materials and Methods

Cells, viruses, and infections. A549 cells and ATCC HeLa cells were grown in Dulbecco's modified Eagle medium supplemented with 10% calf serum at 37^{o}C in 5% CO_2. The viruses used, which were purified on CsCl equilibrium gradients, are dl309 (phenotypically wild type Ad5) (67, 101), dl355 (E4-ORF6 mutant) (60), inORF3 (E4-ORF3 mutant) (60), dl1520 (E1B-55K mutant) (9), dl355/inORF3 (E4-ORF6 and E4-ORF3 double mutant) (60), and dl1520/dl341 (E1B-55K and E4-ORF3 double mutant) (124). Virus particle concentration was determined by obtaining the optical density (OD) at 260nm and multiplying by $1x10^{12}$ particles per milliliter. Infections were performed at 200 virus particles per cell (10 infectious units per cell) for 1h followed by replacement with media and incubation at 37^{o}C in 5% CO_2. In some cases, cells were treated with cytosine arabinoside (AraC) at 25 μg/ml or α-amanitin at 20 μg/ml by adding it to the replacement media.

Viral DNA replication assay. A549 cells were infected for various time points and lysates were subsequently prepared by resuspending infected cells in isotonic buffer (150 mM NaCl, 10 mM Tris [pH 7.4], 1.5 mM $MgCl_2$) and containing 0.6% NP-40. The samples were incubated on ice for 10 min, followed by centrifugation at 800 x g for 5 min to pellet nuclei. Nuclei were then resuspended in SDS lysis buffer (0.5% SDS, 200 mM Tris [pH 8.0], 50 mM EDTA, 0.1 mg/ml proteinase K) and incubated at 55^{o}C overnight. The samples were subsequently subjected to phenol/chloroform extraction, the DNA was ethanol precipitated, and resuspended in TE (10 mM Tris [pH 8.0], 1 mM EDTA) overnight at 4^{o}C. Samples were standardized by measuring absorbance at 260nm and diluted as follows in TE. The time points 4-12 h post-infection (hpi) were diluted at 1:10, 15 hpi at 1:100, 18 hpi. at 1:200, and 24 hpi at 1:300. The DNA was denatured in 0.3 N NaOH for 1 hour at 65^{o}C and then neutralized in 2 M ammonium acetate. The samples were then applied to Hybond N+ (Amersham) with a slot blot apparatus. The DNA was crosslinked using a Stratalinker (Stratagene) and subjected to Southern hybridization with a ^{32}P-labeled probe made by random priming with the

whole Ad5 genome (44). The DNA was visualized on an ABI Storm 860 Phosphorimager and quantified using Image Quant 1.1 software (Molecular Dynamics).

Immunoblots. Whole cell extracts were prepared by resuspending infected cells in SDS lysis buffer (1.2% SDS, 150 mM Tris [pH 6.8], 30% glycerol) and boiling for 10 min. The samples were centrifuged at 16.1 x g for 30 min, supernatants were collected, and the total protein concentration was determined using Pierce BCA method. Standardized amounts of protein were subjected to 12.5% SDS-PAGE, transferred to nitrocellulose, and blocked in 1% casein in TBS. Each membrane was probed with an anti-γ tubulin rabbit polyclonal antibody (Sigma) at 1:5000 and one of the following antibodies at 1:1000: anti-Mre11 mouse monoclonal (Genetex), anti-Rad50 mouse monoclonal (Novus), or anti-Nbs1 mouse monoclonal (Genetex). The secondary antibodies, IR680 goat anti-mouse and IR800 goat anti-rabbit (LiCor) were used and the proteins were detected and quantified using the Odyssey Infrared Imaging System (LiCor). For cell fractionation experiments, infected cells were resuspended in hypotonic buffer (10 mM Tris [pH 7.4], 10 mM NaCl, protease and phosphatase inhibitors), incubated on ice for 10 min, followed by 20 strokes of Dounce homogenization and centrifugation at 800 x g for 5 min. The supernatant contained the cytoplasmmic fraction. The pellets contained the nuclear fraction and were resuspended in RIPA buffer (50 mM Tris [pH 8.0], 150 mM NaCl, 1% NP-40, 0.1% SDS, 0.5% deoxycholic acid, protease and phosphatase inhibitors), incubated on ice for 20 min, spun at 16.1 x g for 20 min and the supernatant collected. The total protein concentration of each fraction was determined, as described above. Standardized amounts of protein were subjected to 12.5% SDS-PAGE, transferred to Hybond P (Amersham), and blocked in 3% BSA in PBS. The membranes were probed using anti-Mre11 rabbit polyclonal antibody (Novus) at 1:5000, anti-Rad50 mouse monoclonal antibody (Genetex) at 1:1000, and anti-Nbs1 rabbit polyclonal antibody (Novus) at 1:10,000. HRP conjugated

secondary antibodies were used and the proteins were detected using enhanced chemiluminescence (Amersham).

Immunofluorescence. A549 and HeLa cells were seeded on glass coverslips and transfected according to the manufacturers instructions using Fugene 6 (42) and/or infected, as described above. In some cases, the cells were then exposed to 1 Gy of ionizing radiation from Cs at 10 hpi. At times indicated in the text, the cells were washed with PBS, fixed with -20^{o}C methanol for 5 min, and washed again with PBS. The cells were blocked in 10% goat serum diluted in PBS and then incubated with primary antibodies diluted in 10% goat serum. The antibodies used were: anti-DBP mouse monoclonal (generous gift of Dr. Arnold Levine, Princeton University) at 1:50, anti-Mre11 rabbit polyclonal (Novus) at 1:600, anti-Rad50 rabbit polyclonal (Novus) at 1:600, anti-Nbs1 rabbit polyclonal (Novus) at 1:1200, and anti-phosphoATM-S1981 rabbit polyclonal (Rockland) at 1:1,000, anti-Adenovirus protein VII rabbit polyclonal (generous gift of Dr. Daniel Engel, University of Virginia) at 1:1,000, anti-γH2AX-S139 rabbit polyclonal (Upstate) at 1:300, and anti-Mdc1 rabbit polyclonal (Bethyl) at 1:500. The cells were washed and incubated with appropriate secondary antibody. Combinations of AlexaFluor 350-conjugated (Molecular Probes), fluorescein isothiocyanate (FITC)-conjugated (Zymed), and tetramethyl rhodamine isothiocyanate (TRITC)-conjugated (Zymed) goat anti-mouse or rabbit IgG antibodies were used. The cells were washed a final time and mounted on slides with Immu-Mount (Thermo Shandon). The microscope used was a Zeiss Axiovert 200M Digital Deconvolution Microscope fitted with a Chroma filter set and an apotome and images were captured with a Peltier-cooled CCD Axiocam HRm camera and analyzed with Axiovision 4.5 software.

TP Cleavage Assay. A549 cells were infected and nuclei were isolated using isotonic buffer containing NP40, as described above. Viral DNA was then isolated by the procedure of Hirt (57), however, only half of the sample was treated with proteinase K. DNA was purified on a Qiagen PCR MinElute column, digested with *Bgl*II, separated on a 1% agarose gel, and analyzed by

Southern hybridization with a ^{32}P-labeled Ad5 total genome probe made by random primer labeling (44). Pixel intensities were measured on the ABI Storm 860 Phosphorimager (Molecular Dynamics) and quantified using ImageQuant 1.1 software (Molecular Dynamics).

Click-iT EdU Assay. The Click-iT™ EdU Alexa Fluor High-Throughput Imaging (HCS) Assay kit was used to label viral DNA *in situ* (Invitrogen). dl355/inORF3 virus was grown in regular media for 18 hrs and then the media was replaced with media that contained the nucleoside analog of thymidine, EdU (5-ethynyl-2'-deoxyuridine) at 10 μM. This nucleotide was incorporated into the viral DNA and packaged into virions. The virions were purified as described earlier and used to infect A549 cells. After fixation, the cells were stained using an AlexaFluor 488-azide, which forms a covalent link to the EdU that is incorporated in the viral DNA. Extensive washes with 10% goat serum were performed, followed by immunostaining as previously described.

Results

Time course of MRN degradation compared to viral DNA replication during Ad infection.

In the literature, the earliest decrease in levels of the MRN complex during an Ad infection is at 12-16 hpi (87, 133). To examine this in A549 cells, a time course was performed in which cell lysates were prepared from mock-infected cells and inORF3-infected cells at 6, 8, 10, 12, 14, and 18 hpi and MRN levels were measured by quantitative Western blot analysis using antibodies against Mre11, Rad50, and Nbs1. γ-tubulin levels were measured to normalize each sample. Mutant inORF3 (lacking E4-ORF3) was used for this analysis so that only the E1B-55K–E4-ORF6 complex contributes to MRN regulation. At 6 and 8 hpi, the levels of the components of the MRN complex were similar or slightly greater than the levels in mock-infected cells (Fig. 1). By 10 and 12 hpi however, the Mre11 and Rad50 signals were diminished by about half. Significant degradation of these proteins was observed by 18 hpi. As seen previously in the literature, Nbs1 protein levels decrease at a reduced rate (4, 133).

Since it is not known if it is important for the MRN complex to be inhibited prior to the onset of viral DNA accumulation, I wished to determine an accurate time point for the beginning of viral DNA replication in Ad-infected A549 cells. I analyzed viral DNA levels during a time course from cells infected with phenotypically wild type Ad5 (dl309) and mutant viruses deleted for E4-ORF6, E4-ORF3, or both proteins (dl355, inORF3, or dl355/inORF3, respectively) starting at 4 hpi until 24 hpi (Fig. 2). Wild type and dl355 viral DNA began to accumulate starting at 10 hpi. Mutant inORF3 grew with similar kinetics but showed a slight lag in the onset of replication. The double mutant, dl355/inORF3, which has a viral DNA replication defect (60), was significantly delayed for viral DNA replication. I conclude that significant levels of degradation of the MRN complex does not occur prior to the accumulation of viral DNA when looking at a population of infected cells.

Figure 1.

MRN degradation does not occur until late during Ad infection. Cell lysates from mock-infected A549 cells and mutant inORF3-infected (E4-ORF3 mutant) A549 cells were harvested at 6, 8, 10, 12, 14, and 18 hpi. **A**. MRN degradation was visualized by immunoblot analysis of each component of the MRN complex along with g-tubulin as a loading control. **B**. Each band was quantified and normalized to γ-tubulin. The values for mock-infected samples are set at 1. Relative levels of Mre11, Rad50 and Nbs1 in infected cell lysates are shown at the indicated time points. The results represent the average of three independent experiments.

A

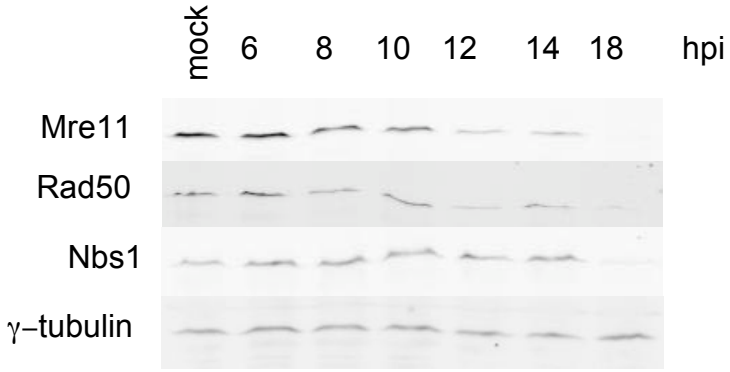

B

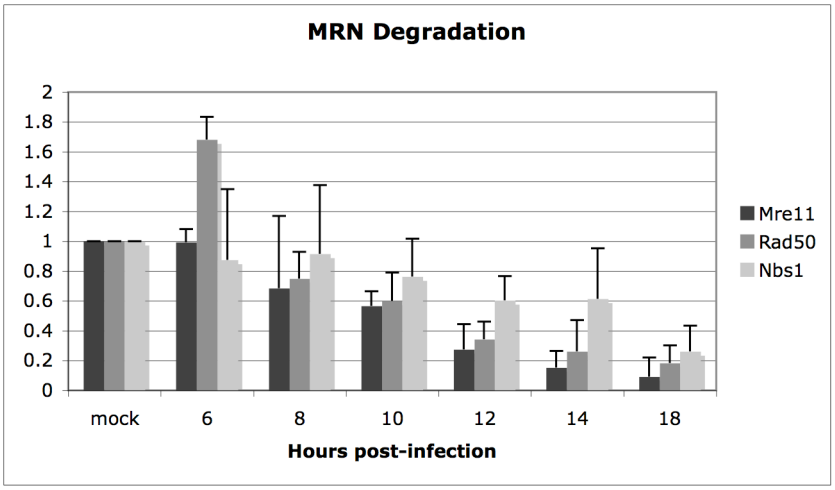

Figure 2.

The onset of viral DNA replication occurs 10-12 hpi with viruses that inactivate MRN. Cells were infected with dl309 (phenotypically wild type Ad5), dl355 (E4-ORF6 mutant), inORF3, or dl355/inORF3 (E4-ORF6/E4-ORF3 mutant). High molecular weight DNA was prepared from infected cell lysates at 4, 6, 8, 10, 12, 15, 18, and 24 hpi. Levels of DNA in each sample were quantified by slot blot analysis and plotted on the graph. Equivalent levels of viral DNA were observed with the 4 and 6 hpi samples compared to the 8 hpi sample. The results represent the average of three independent experiments.

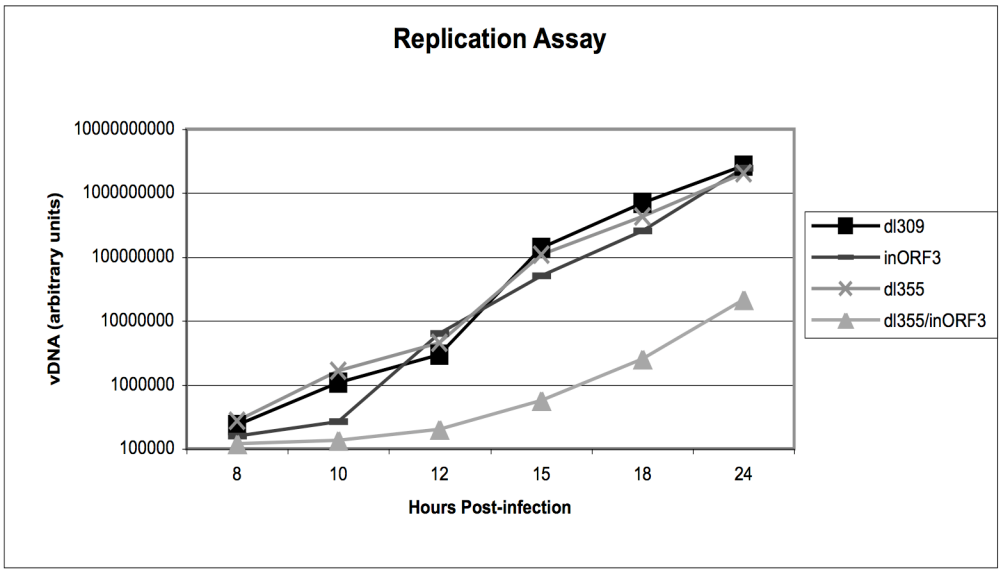

Localization of the MRN complex early during infection.

It seems counterintuitive that total MRN protein levels were not significantly reduced at 10 hpi (Fig. 1) while viral DNA accumulation began (Fig. 2). One would expect that the MRN complex would need to be rendered inactive by the time viral DNA replication began to avoid the inhibition seen on viral DNA replication when the MRN complex is not inactivated. One possible explanation for this apparent contradiction is a relocalization of the MRN complex that renders it functionally inactive, such as to the cytoplasm, which is in line with the reported transport of Mre11 into cytoplasmic aggresomes (4, 87). E4-ORF3 is known to function similarly by relocalizing the MRN complex within the nucleus to inhibit the activity. For this reason, I determined the localization of the MRN complex early during Ad infection. I utilized subcellular fractionation to determine if the MRN complex was relocalized from the nucleus to the cytoplasm in infected A549 cells. Nuclear and cytoplasmic fractions of cell lysates made at 8 hpi following infection with several mutant viruses were analyzed by Western blot using antibodies against Mre11, Rad50, and Nbs1 (Fig. 3). There was no difference in the nuclear versus cytoplasmic accumulation of these proteins in mock-, dl355-, inORF3-, or dl355/inORF3-infected cells.

Degradation of the MRN complex occurs before the accumulation of viral DNA.

Immunofluorescence experiments also were performed to visualize the localization of the MRN complex in infected cells. An E4 mutant was used that does not express a functional E4-ORF3 protein to prevent MRN relocalization and functional inactivation in order to directly assess MRN regulation by E1B-55K–E4-ORF6. Cells were infected with mutant inORF3 and then immunostained at 8 hpi with antibodies against DBP and Mre11, Rad50, or Nbs1. In about 75% of DBP-positive cells at 8 hpi, the signal for each of the components of the MRN complex decreased (Figs. 4 and 8). The decrease in signal was dependent on both E1B-55K and E4-ORF6 as seen by a return in signal in nearly 100% of cells infected with viruses that

Figure 3.

There is no significant relocalization of the MRN complex early after Ad infection. Mock-infected A549 cells or A549 cells infected with dl355, inORF3, or dl355/inORF3 for 8 h were fractionated into nuclear and cytoplasmic samples and subjected to immunoblot analysis with antibodies against Mre11, Rad50, and Nbs1.

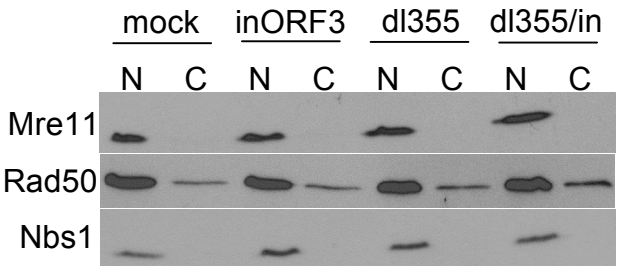

Figure 4.

Immunofluorescence microscopy shows a disappearance in MRN signal by 8 hpi. A549 cells were infected with inORF3. The cells were then fixed and stained with antibodies for Mre11, Rad50, or Nbs1 (FITC, green) and DBP (Alexa Fluor 350, blue). Images were captured using a deconvolution microscope.

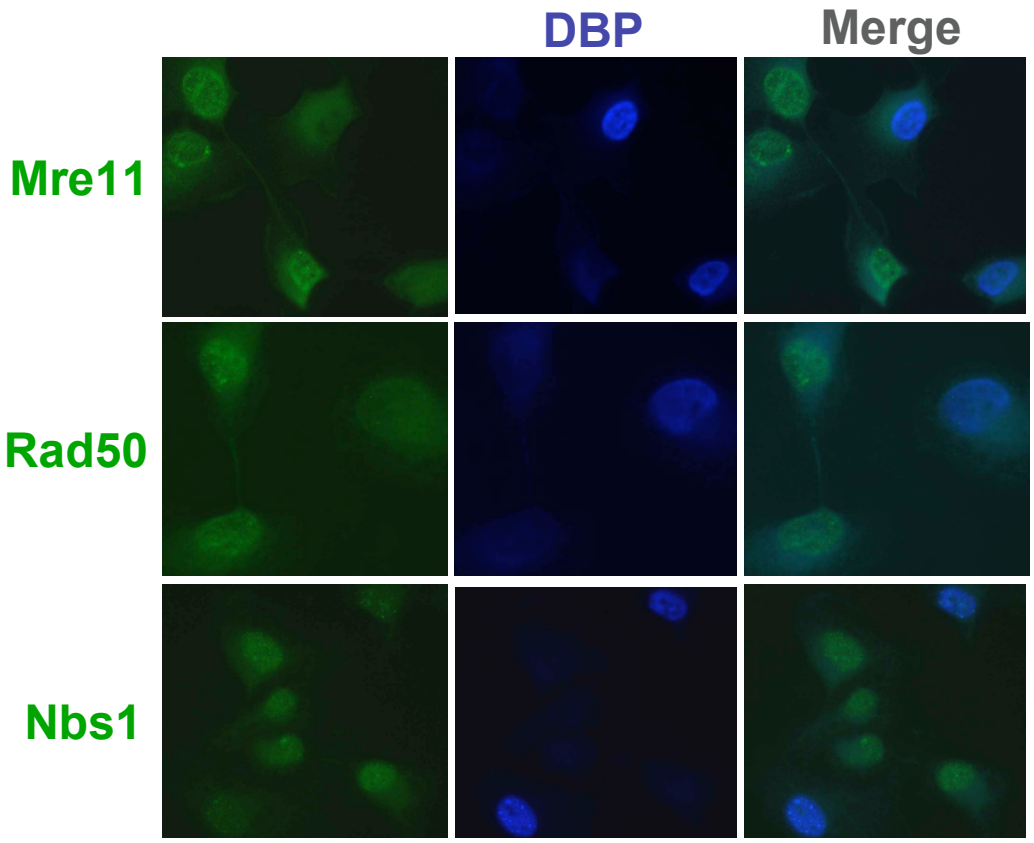

Figure 5.

Immunofluorescence microscopy shows a disappearance in MRN signal by 8 hpi that is dependent on E4-ORF6. A549 cells were infected with dl355/inORF3. The cells were then fixed and stained with antibodies for Mre11, Rad50, or Nbs1 (FITC, green) and DBP (Alexa Fluor 350, blue). Images were captured using a deconvolution microscope.

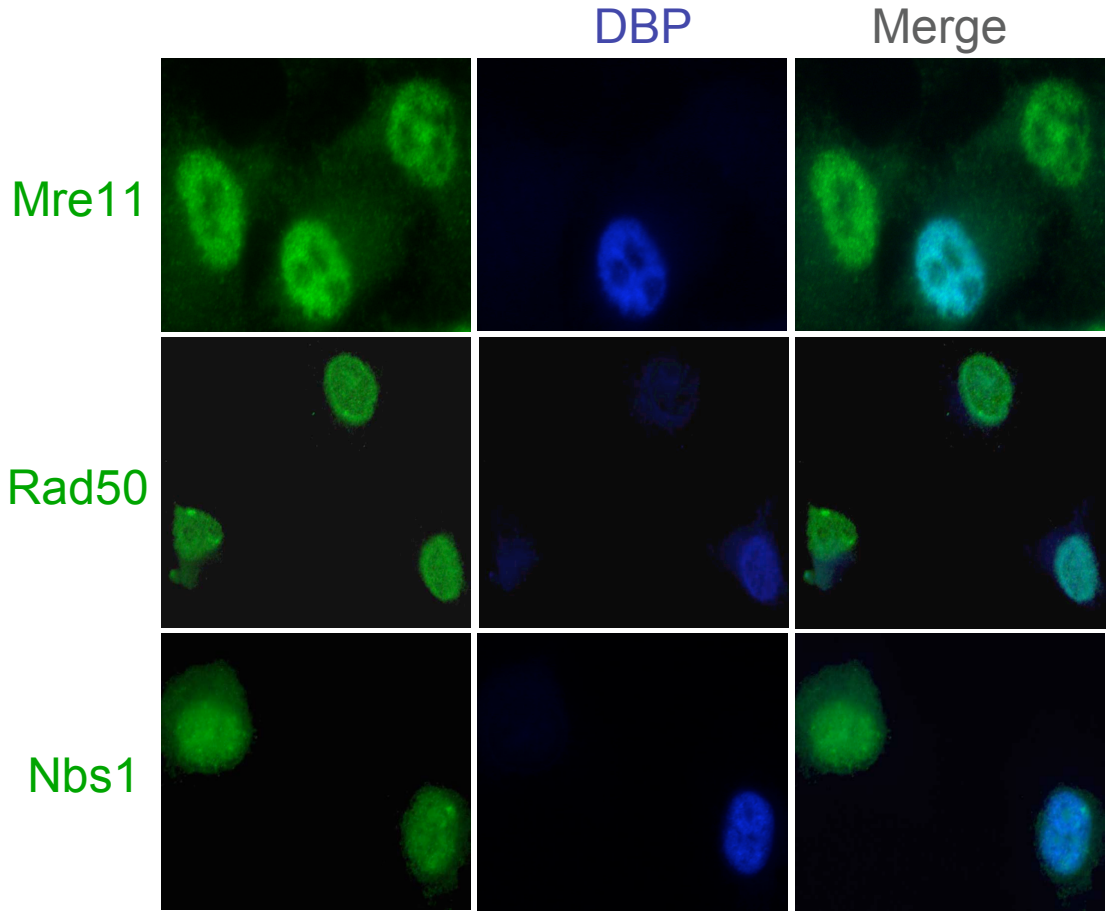

Figure 6.

Immunofluorescence microscopy shows a disappearance in MRN signal by 8 hpi that is dependent on E1B-55K. A549 cells were infected with dl355/inORF3. The cells were then fixed and stained with antibodies for Mre11, Rad50, or Nbs1 (FITC, green) and DBP (Alexa Fluor 350, blue). Images were captured using a deconvolution microscope.

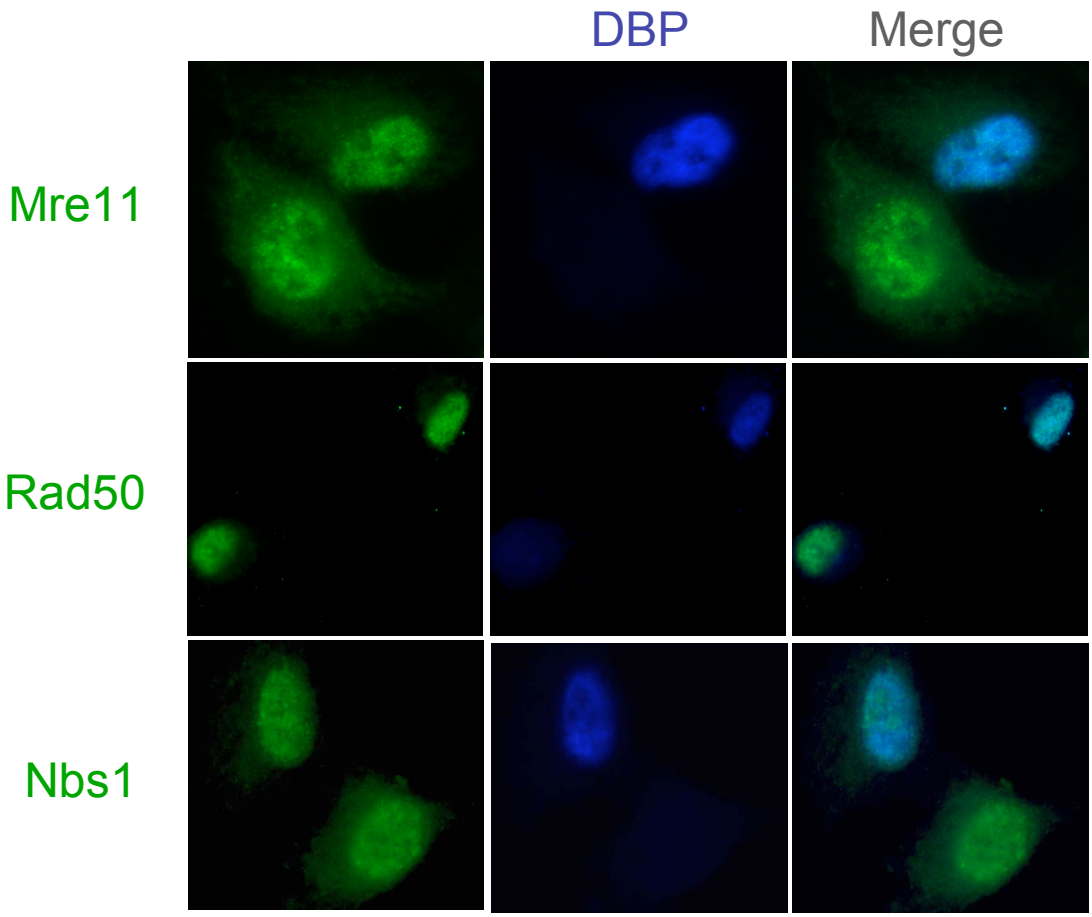

lacked a functional E4-ORF3 and E4-ORF6 (dl355/inORF3) or E1B-55K (dl1520/dl341) (Fig. 5, 6, and 8). Since the loss of MRN signal was observed at 8 hpi whereas viral DNA replication in mutant inORF3-infected cells was only evident between 10-12 hpi (Fig. 2), I conclude that MRN is degraded in Ad-infected cells prior to viral DNA accumulation.

If the disappearance in MRN signal in the immunofluorescence assays was in fact due to degradation, there appeared to be a discrepancy in the timing of the degradation during Ad infection when comparing the results of biochemical methods (Fig. 1) with immunofluorescence assays (Figs. 4-6, and 8). One difference between these two methodologies is that the biochemical assay looks at a population of cells while the immunofluorescence is a single cell-based assay. During an infection, different cells may progress through the viral life cycle at different rates and this may cause a difference in results when looking at time-sensitive data in a population versus a single cell. To determine if this was the reason for the apparent discrepancy, a single-cell assay was implemented to visualize MRN degradation.

I utilized a dominant-negative Cullin 5 mutant (159) to determine if the disappearance in MRN signal using immunofluorescence was due to proteasomal-dependent degradation. Cullin 5 is a component of the E3 ubiquitin ligase complex that E4-ORF6 and E1B-55K target. Woo and Berk showed that the N-terminal domain (NTD) of CUL5 can prevent the degradation of Mre11 during Ad infection (159). I co-transfected cells with the CUL5-NTD expression plasmid and a DsRed-mito expression plasmid, as a marker of transfected cells. Subsequently, the cells were infected with mutant inORF3 and immunostained at 8 hpi with antibodies against DBP and Mre11. In 91% of cells that had been transfected (DsRed-mito-positive) and were DBP-positive, the Mre11 signal was restored (Figs. 7 and 8) indicating that the loss of signal seen during mutant inORF3 infection is due to the degradation of Mre11 in these cells.

Figure 7.

Disappearance of Mre11 signal is dependent on the Cullin5-containing E3 ubiquitin ligase complex. A549 cells were co-transfected with CUL5-NTD and DsRed2-mito expression plasmids overnight and infected with inORF3 for 8 h. The cells were then fixed and stained with antibodies for Mre11 (FITC, green) and DBP (Alexa Fluor 350, blue). Images were captured using a deconvolution microscope.

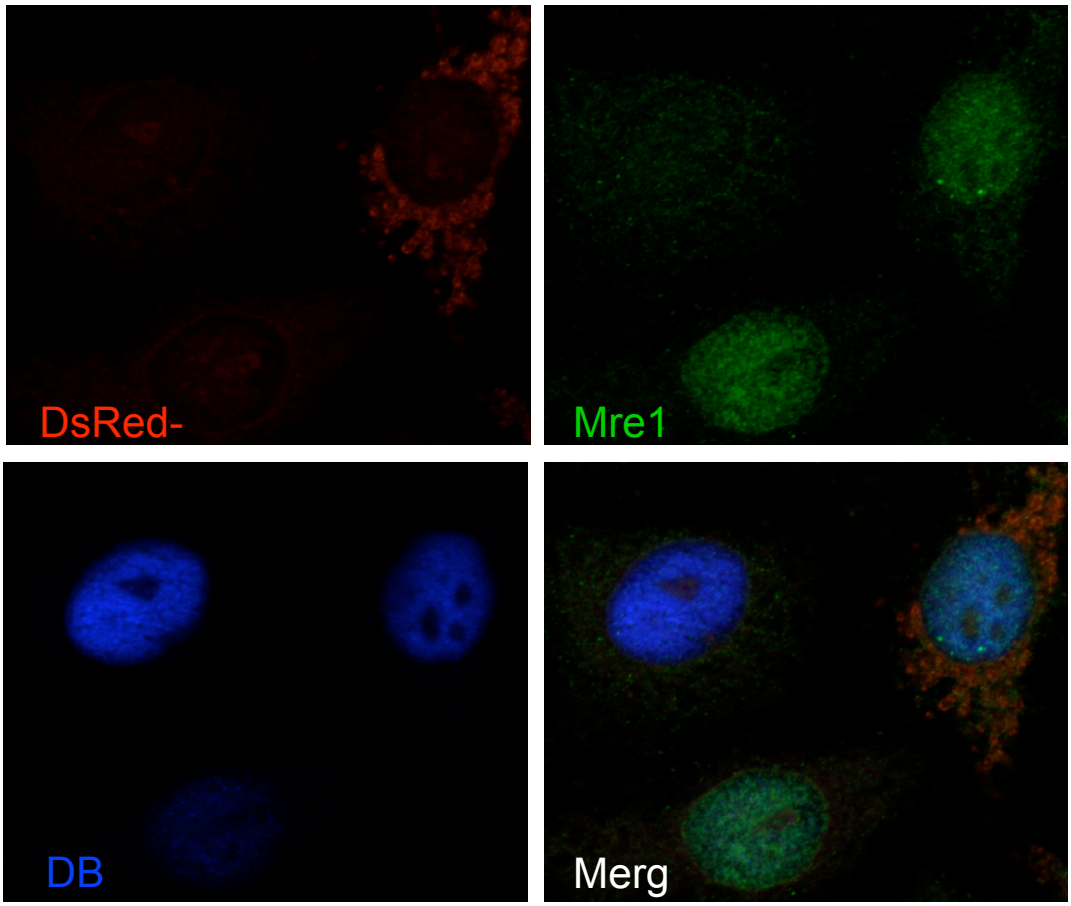

Figure 8.

Immunofluorescence microscopy shows a disappearance in Mre11 signal by 8 hpi that is due to degradation by E4-ORF6 and E1B-55K. A549 cells were infected with inORF3, dl355/inORF3, dl1520/dl341, or co-transfected with CUL5-NTD and DsRed2-mito expression plasmids overnight and infected with inORF3 for 8 h. The cells were then fixed and stained with antibodies for Mre11 and DBP. Images were captured using a deconvolution microscope. Cells were scored positive or negative for Mre11 for staining and the percentages of 50 cells in triplicate were plotted on the graph.

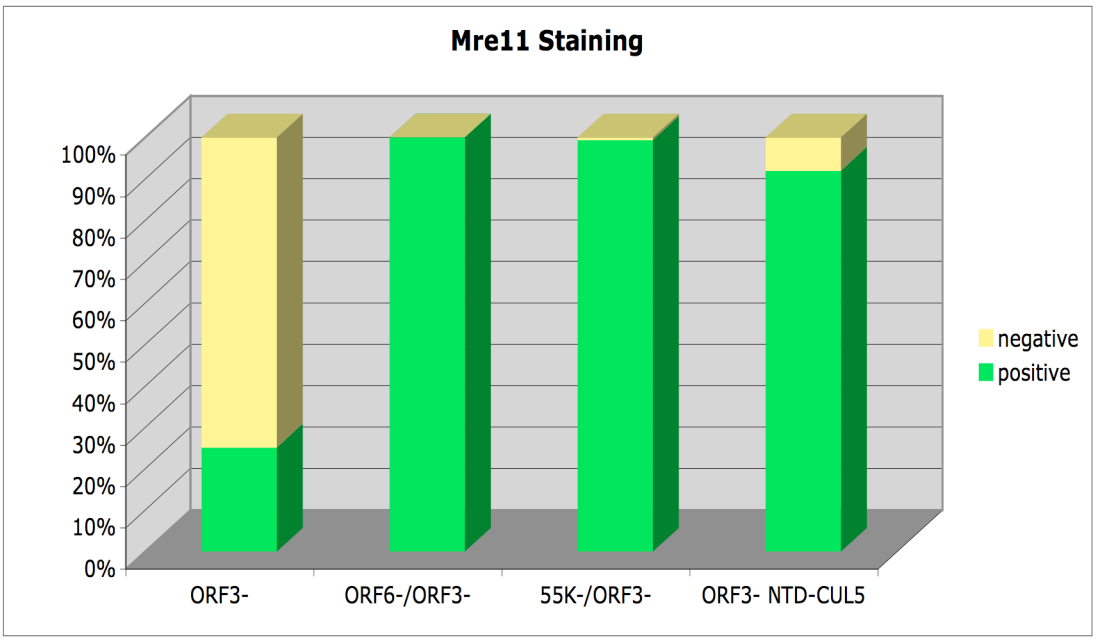

The MRN complex is functionally inhibited by E4-ORF3 and E1B-55K–E4-ORF6 at the onset of replication.

To examine MRN degradation on a single cell basis in Ad-infected A549 cells, I used checkpoint signaling, as seen by phospho-ATM (pATM) focus formation, as an indication of MRN function. MRN activity is required for the induction of pATM foci following the induction of DNA damage (79). I costained Ad-infected cells at 10 hpi for the Ad DNA binding protein (DBP) and ATM phosphorylated at S1981 (pATM) and counted the number of pATM-S1981 foci that formed in DBP-positive cells (Fig. 9 and 10). DBP is an early viral protein and served as a marker for infected cells.
With mock-infected cells, very few pATM foci were evident (Fig. 9 A, D). Similarly, in cells infected with dl309, dl355, inORF3, or dl1520 (an E1B-55K mutant), very few pATM foci were observed suggesting that there was significant protection of the viral genomes from detection by the MRN complex and subsequent checkpoint signaling by 10 hpi (Fig. 9 B, D). In contrast, the two double mutants, dl355/inORF3 and dl1520/dl341 (an E1B-55K, E4-ORF3 double mutant), had a significant number of pATM foci with an average of ~10 per cell (Fig. 9 C, D). Taken together, these results show that when either E4-ORF3 or the combination of E1B-55K and E4-ORF6 are present, they functionally inhibit the MRN complex and prevent checkpoint signaling elicited by the recognition of viral genomes. The increase in pATM foci observed in cells infected with the replication-defective double mutants compared to the mock-infected cells strongly indicates that the input viral genomes from the initial infection are sufficient to induce MRN signaling.

Infected cells were also irradiated with 1 Gy of ionizing radiation (IR) at 10 hpi, fixed at 1 hour post-irradiation, and stained for DBP and pATM. In mock-infected, irradiated cells, there was an average of ~12 pATM foci per cell (Fig. 10 E, H). Wild type virus (dl309) was able to strongly inhibit checkpoint signaling with only ~3 foci per cell, even after exogenously-introduced DSBs were formed (Fig. 10 F, H). Each of the single mutants (dl355, inORF3, and dl1520) were able to prevent a full checkpoint signaling

Figure 9.

The MRN complex is inactivated by 10 hpi in wild type and single mutant infections. A549 cells were mock-infected (**A**) or infected with dl309 (**B**), dl355, inORF3, dl1520 (E1B-55K mutant), dl355/inORF3 (**C**), or dl1520/dl341 (E1B-55K/E4-ORF3 mutant) for 10 h. The cells were then fixed and stained with antibodies against DBP and pATM-S1981 using Alexa Fluor 350 (blue) or FITC (green), respectively, for detection. **A-C** show representative immunofluorescence images. (**D**) The number of pATM foci were counted in DBP-expressing cells for 50 cells each virus in triplicate and the average was plotted in the graphs. The results represent the cumulative value of pATM foci observed; ie. 0 represents the number 1 of cells with 0 pATM foci, 1 represents the number of cells with 0 and 1 pATM foci, 2 represents the number of cells with 0, 1 and 2 pATM foci, etc. P values were determined for each virus as compared to mock using the Mann-Whitney test (* $p<0.05$, ** $p<0.001$).

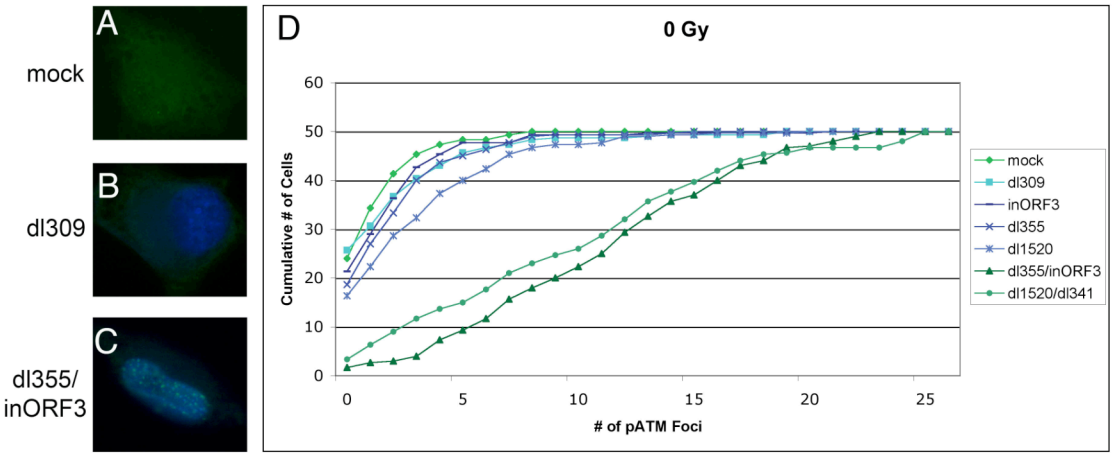

Figure 10.

The MRN complex is inactivated by 10 hpi in wild type and single mutant infections even after exposure to IR. A549 cells were mock-infected (**E**) or infected with dl309 (**F**), dl355, inORF3, dl1520 (E1B-55K mutant), dl355/inORF3 (**G**), or dl1520/dl341 (E1B-55K/E4-ORF3 mutant) for 10 h. The cells were then treated with 1 Gy of ionizing radiation and fixed 1 h post-irradiation. The cells were stained with antibodies against DBP and pATM-S1981 using Alexa Fluor 350 (blue) or FITC (green), respectively, for detection. **E-F** show representative immunofluorescence images. (**H**) The number of pATM foci were counted in DBP-expressing cells for 50 cells each virus in triplicate and the average was plotted in the graphs. The results represent the cumulative value of pATM foci observed; ie. 0 represents the number 1 of cells with 0 pATM foci, 1 represents the number of cells with 0 and 1 pATM foci, 2 represents the number of cells with 0, 1 and 2 pATM foci, etc.

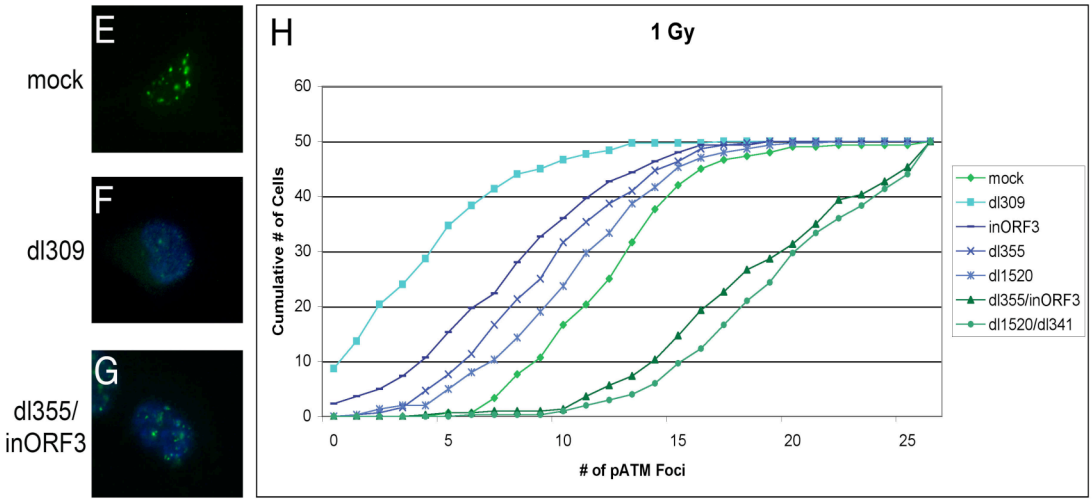

response with ~7-10 foci per cell (Fig. 10H). Both double mutants (dl355/inORF3 and dl1520/in341) were unable to inhibit checkpoint signaling and ~18 pATM foci formed per cell (Fig. 10 G, H). These results demonstrate that by 10 hpi, checkpoint signaling is not only inhibited for recognition of viral genomes in wild type and single mutant infections, but also for DSBs in cellular chromatin induced by ionizing radiation. Once again the comparison of the results using the mock versus double mutant virus infections supports the conclusion that the input viral genomes are sufficient to induce a DSBR response.

Terminal protein cleavage is not the basis for MRN inhibition of Ad replication.

In order to visualize the nucleolytic processing that is thought to occur prior to Ad genome concatenation, an assay was utilized to determine if TP is cleaved off the viral genome by 10 hpi during an infection with viral mutants that are unable to inhibit the MRN complex. I sought to determine if endonucleolytic cleavage of the genome removed TP. Nuclear DNA was analyzed from virus-infected cells so as to exclude the viral genomes that entered the cell, but failed to travel to the nucleus. Hirt extraction was performed (57) using 0.6% SDS and 0.75M NaCl in the lysis buffer, which disturbed many of the non-covalent interactions between the viral DNA and other proteins. Half of these extracts were treated with proteinase K and all samples were digested with the restriction enzyme *Bgl*II. The samples were separated on an agarose gel and subjected to Southern blot analysis with a ^{32}P-radiolabeled Ad5 whole genome probe. The terminal fragments that were treated with proteinase K will not have TP attached and will run at 3327 bp and 1543 bp for the left and right termini, respectively, with the exception of the left end fragments for the dl1520 mutants. The deletion made in this mutant removed the *Bgl*II site and created a terminal fragment of about 8 kb. For the samples that were not treated with proteinase K, TP will be covalently linked and will cause the fragment to remain in the well of the gel. By comparing the quantity of terminal fragment in each sample, the percentage

Figure 11.

TP cleavage is not the basis for MRN inhibition of Ad replication. A549 cells were infected with dl309 (lanes 3-4), dl355 (5-6), inORF3 (7-8), dl1520 (9-10), dl355/inORF3 (11-12), and dl1520/dl341 (13-14), and harvested at 10 hpi to prepare nuclear viral DNA. Part of the samples were treated with proteinase K (odd lanes, indicated +) while the others were left untreated (even lanes, indicated -). The samples were digested with *Bgl*II, run on a 1% agarose gel, and subjected to Southern blot analysis with a ^{32}P-labeled whole genome probe. Standards were run alongside the samples (lanes 1-2). The * align with the terminal fragments - right at 1543 bp, left at 3327 bp except for dl1520 mutants which are about 8 kb. The two arrows represent the terminal (top) and internal (bottom) bands that were compared.

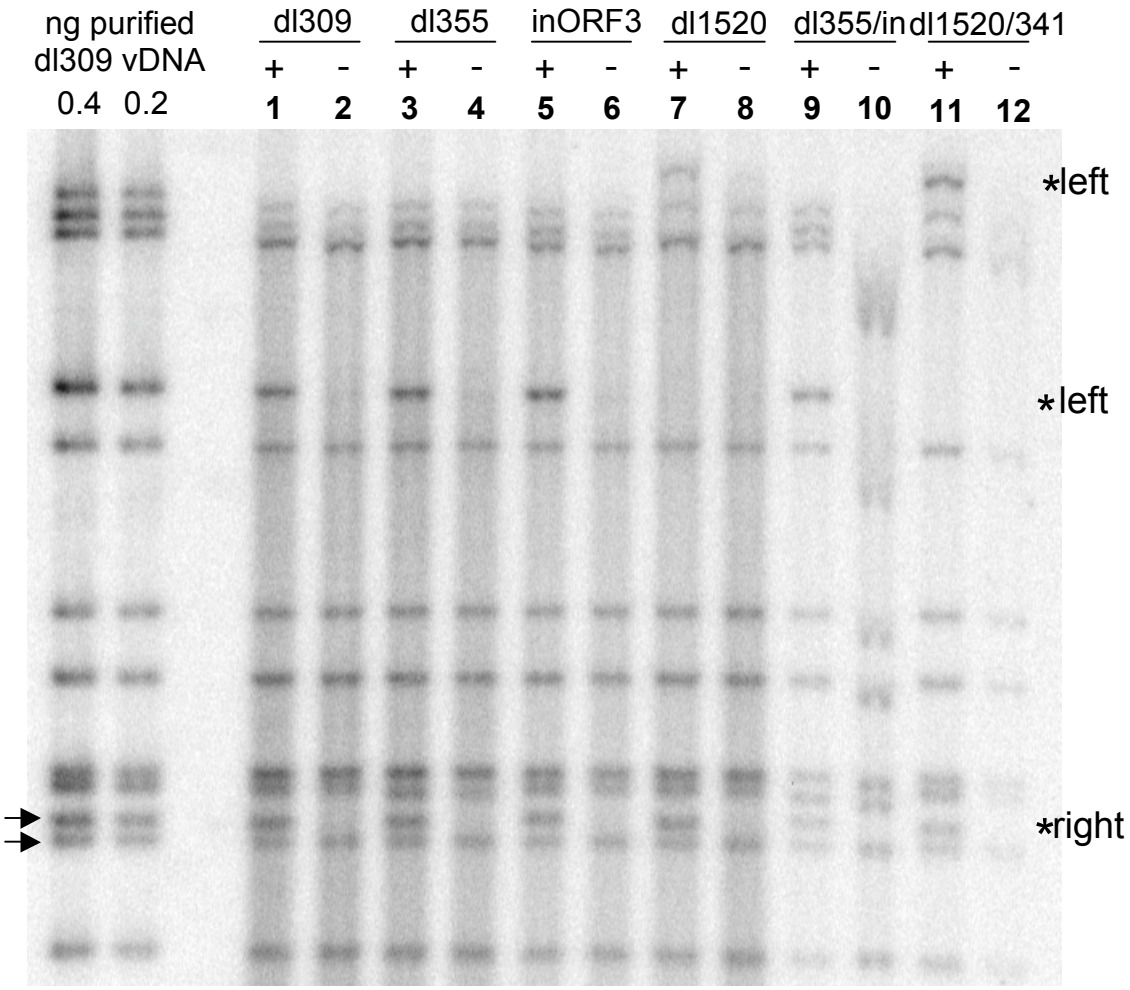

(dl309) and the single mutants (dl355, inORF3, dl1520) indicating that TP was bound (Fig. 11). Similarly, there was a decrease in the non-proteinase K-treated samples with the double mutants (dl355/inORF3 and dl1520/dl341), confirming that TP is still covalently bound to the viral genome at 10 hpi even in the presence of a functional MRN complex. Additionally, with all of the proteinase K-treated samples, the terminal DNA fragments displayed the same apparent mobility in the gel even in the presence of functional MRN. I conclude that neither TP cleavage nor significant nucleolytic cleavage of the viral termini is the basis for MRN inhibition of Ad DNA replication.

pATM foci formed in double mutant infections do not colocalize with Ad protein VII.

In order to further convince ourselves that the pATM foci seen during a double mutant infection (dl355/inORF3) are forming at the viral genomes, immunofluorescence was performed with antibodies against pATM and viral protein VII. I expected protein VII to be bound to the viral genome at 10 hpi and to serve as a marker of the viral DNA (161). Unexpectedly, I found that these two proteins did not colocalize (Fig. 12A-C), however, the pATM foci did colocalize with γH2AX (Fig. 12D-F) suggesting that the pATM foci represent normal IRIF-like foci. Since protein VII is only representative of the viral genome, it was more likely that VII is not representing every genome than that checkpoint signaling foci are not forming at the genomes. Interestingly, there was virtually no colocalization between the VII dots and the checkpoint signaling foci suggesting that the two are mutually exclusive.

To visualize the actual Ad genomes at 10 hpi, the Click-iT EdU imaging assay (Invitrogen) was used. Briefly, dl355/inORF3 viral DNA was labeled with EdU molecules, virus particles were purified, and subsequently used to infect A549 cells. At 10 hpi, the cells were fixed and a click reaction created a covalent bond between a fluor-conjugated azide and the alkyne-containing EdU molecule. Cells were then immunostained for either viral protein VII (Fig. 12G-I) or pATM (Fig. 12J-L). Nearly all the VII or pATM dots colocalized with

Figure 12.

Mutually exclusive binding of viral protein VII or pATM to viral DNA. (A-F) A549 cells were infected for 10 hrs with dl355/inORF3, fixed, and immunostained for either pATM-S1981 (FITC, green) and VII (TRITC, red) **(A-C)** or pATM-S1981 (FITC, green) and γH2AX (TRITC, red) **(D-F)**. **(G-L)** A549 cells were infected for 10 hrs with dl355/inORF3-Edu, fixed, treated with Alexa Fluor 488 (green)-azide to label the viral DNA, and immunostained for either pATM-S1981 **(G-I)** or VII **(J-L)** (TRITC, red). Images were captured using a deconvolution microscope.

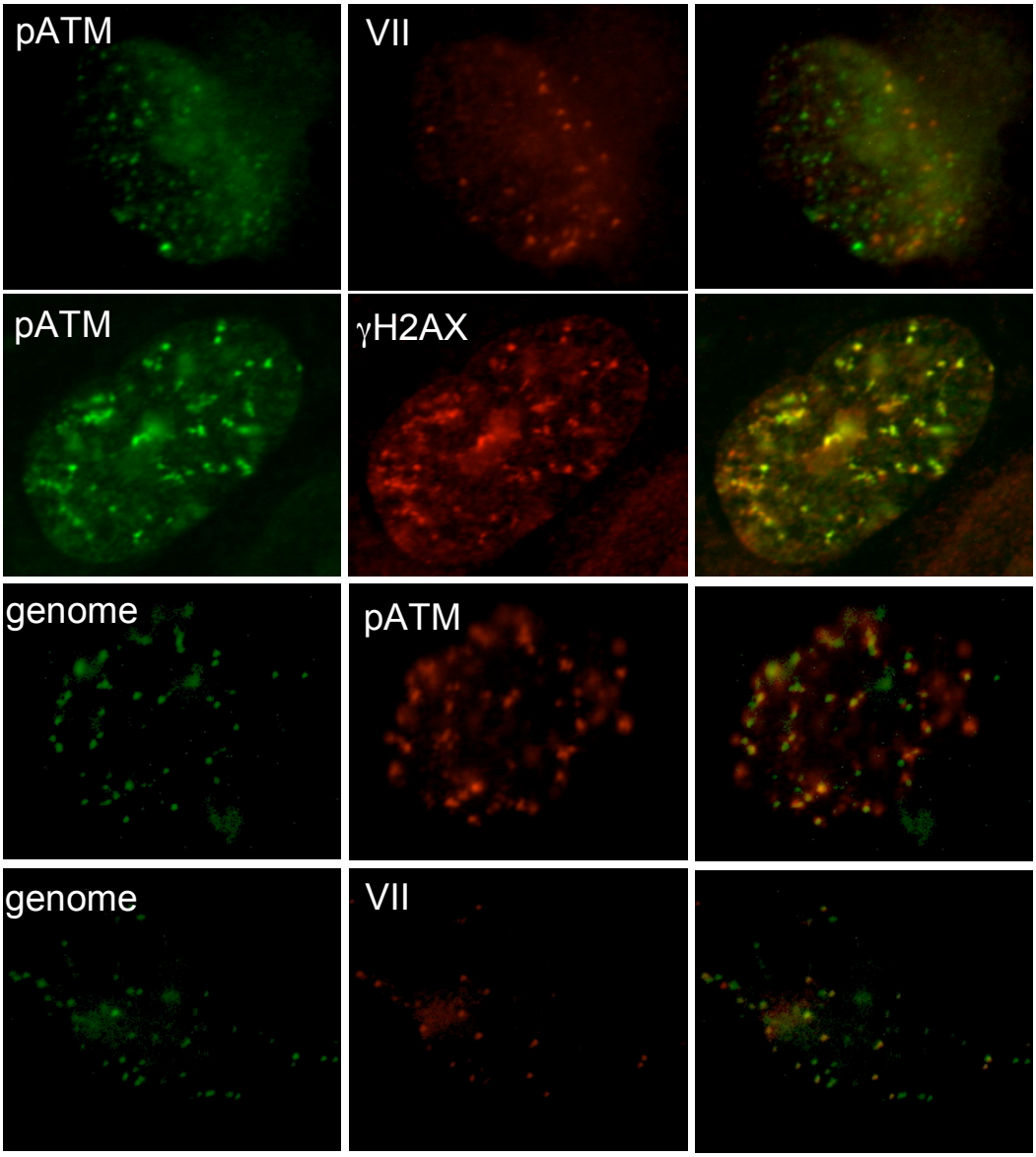

of genomes with TP bound can be determined. As expected, there was a significant decrease in the intensity of the terminal bands in the non-proteinase K-treated samples for wild type the EdU-labeled genomes, however, in each case, there were more EdU dots that did not colocalize with the respective protein, suggesting that they were colocalizing with the other protein. This data support the conclusion that while both Ad protein VII and pATM colocalize with viral DNA at 10 hpi, they do not colocalize with each other and represent mutually exclusive viral DNA interactions.

There is a temporal correlation between the loss of VII dots and the gain of pATM foci.

It was recently determined that viral protein VII is released from viral genomes that are undergoing high levels of transcription and that as the infection progresses, the number of VII dots decreases until all of the VII dots disappear by 12 hpi; subsequently, there is weak and diffuse nucleoplasmic staining at around 14 hpi (29). I performed a time course experiment using the double mutant virus, dl355/inORF3, and staining for pATM and protein VII from 2-14hpi. The number of foci from each protein was determined in 50 cells in triplicate and the average was plotted in two graphs (Figs. 13 and 14). In mock-infected cells and up to 4 hpi, there were very few pATM foci present. By 6 hpi, the number of pATM foci began to steadily increase. At 2 hpi, the average number of VII dots is 18, which is as expected for the MOI used. By 6 hpi, the number of VII dots began to decrease. As the infection progresses, the number of VII dots steadily decreased, as the number of pATM foci increases at an inverse rate (Fig. 13). Figure 14 shows that irrespective of the dynamic shift in VII dots to pATM foci, the total number of foci remains level at ~20, suggesting that each focus represents a viral genome.

Inhibition of transcription inhibits pATM formation.

The increase in pATM foci began around 6 hpi, however, the switch from a majority of VII dots to pATM foci occurred around 10 hpi, suggesting that an event occurring at this time triggers the recognition of the viral genomes by the MRN complex. Higher levels of transcription occur at this

Figure 13.

The number of VII dots decreases at an inverse rate as the increase of pATM foci. A549 cells were mock-treated or infected with dl355/inORF3 over a time course of 2-14 hours. The cells were then fixed and immunostained for viral protein VII and pATM. The number of foci for each protein was counted in 50 cells in duplicate by microscopy and the average number was plotted.

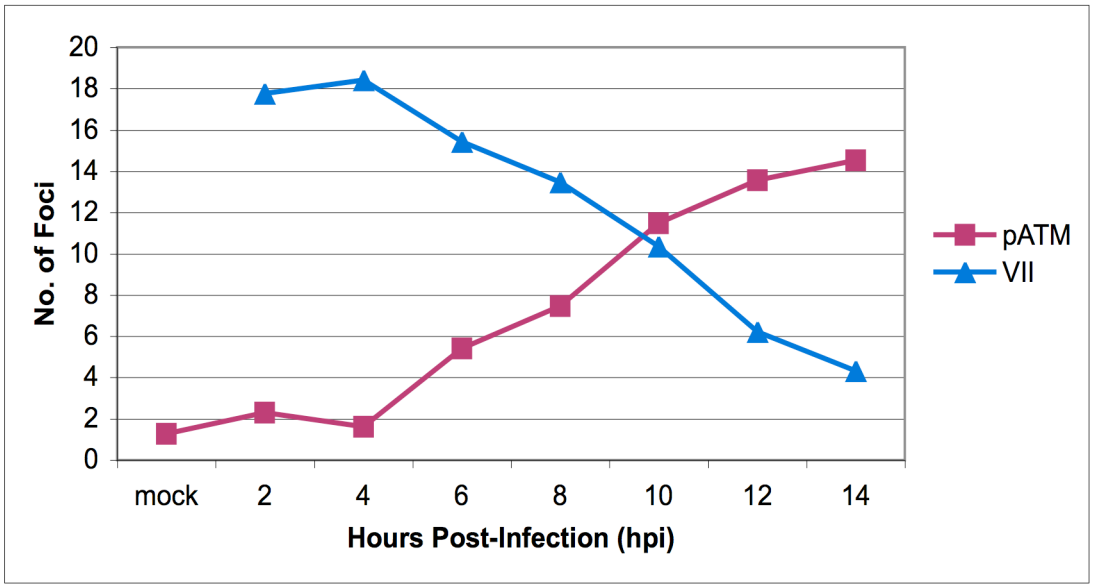

Figure 14.

The total number of VII dots and pATM foci remains the same during an infection. A549 cells were mock-treated or infected with dl355/inORF3 over a time course of 2-14 hours. The cells were then fixed and immunostained for viral protein VII and pATM. The number of foci for each protein was counted in 50 cells in duplicate and the average number of each was plotted.

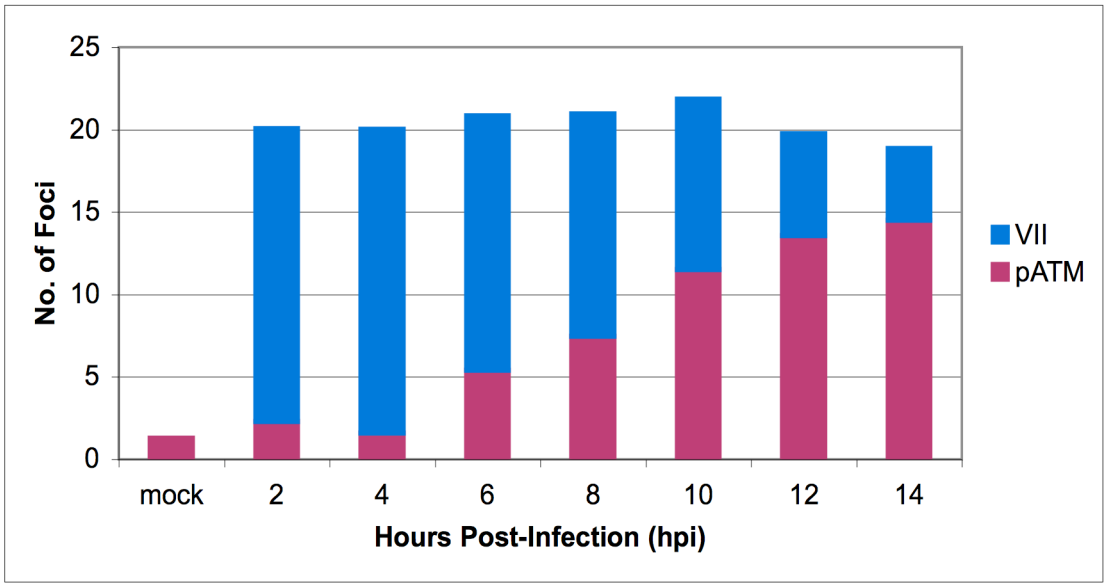

time, and as I have seen, protein VII is released from the viral genome. Engel *et al*. (29) have shown that these two events are connected with VII release being dependent on viral transcription. Viral DNA replication also begins to occur around this time. I performed immunofluorescence experiments to determine whether transcription or DNA replication were involved in the increase in checkpoint signaling. Cells were infected for 10 hours with untreated dl355/inORF3, dl355/inORF3 treated with AraC, dl355/inORF3 treated with α-amanitin, or dl312 (E1A-deleted virus). E1A is the immediate early Ad gene that acts as a transcriptional activator of early region genes (11). An E1A deletion prevents significant levels of transcription from occurring on the viral genomes. The number of pATM foci and VII dots were counted under each condition (Fig. 15). In the untreated dl355/inORF3-infected cells, the average number of pATM foci was about 13 and the VII dots was about 8. After treatment with the DNA replication inhibitor, AraC, the numbers were similar with the pATM foci average around 13.5 and the VII dots about 7. Interestingly, treatment with the transcriptional inhibitor, α-amanitin, or infection with dl312, resulted in an increase in VII dots (about 16.5 for both) as expected, and a decrease in pATM foci (5.4 and 6, respectively). These results show that the inhibition of transcription, but not the inhibition of DNA replication can reduce the amount of checkpoint signaling occurring due to recognition of the genomes by the MRN complex. Since transcription causes the release of viral protein VII from the genome, the presence of VII may be providing protection to the viral genome.

Figure 15.

Inhibition of transcription during an infection can inhibit pATM foci formation. A549 cells were infected with dl355/inORF3 or dl312 (E1A$^-$) for 10 hours. Cells were left untreated or treated with AraC (25 μg/ml) or α–amanitin (20 μg/ml) as the media was replaced following the infection. Cells were fixed and immunostained for viral protein VII or pATM and the number of foci from each protein was counted in 50 cells in triplicate. The average numbers were plotted in the graph below. The error bars represent the 95% confidence interval and the values for the α-amanitin-treated dl355/inORF3-infected cells and the dl312-infected cells are statistically significant from the values for untreated cells ($p < 0.001$).

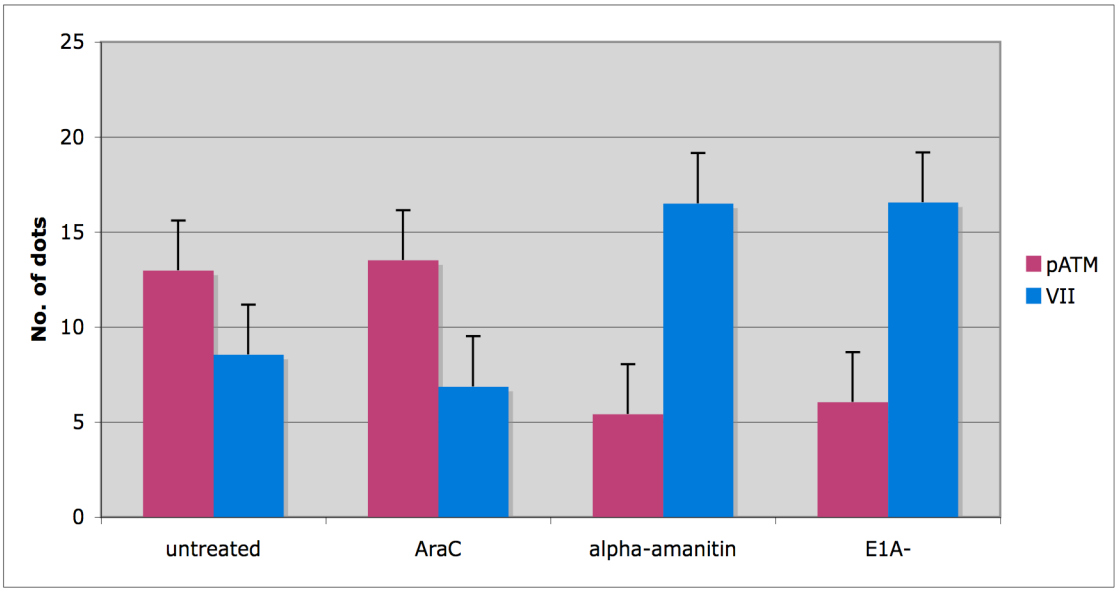

Discussion

The importance of the inhibition of the MRN complex during an Ad infection is illustrated by the redundant mechanisms utilized to inactivate the complex and is seen experimentally by a delay in the onset of virus replication and a significant decrease in viral DNA levels and virus yield with mutants that lack the ability to inhibit the MRN complex (16, 54, 60, 153). The E4-ORF3 protein is responsible for one mechanism in which the MRN complex is sequestered into nuclear inclusions by 6 hpi (45, 133, 134). The E1B-55K and E4-ORF6 proteins form an E3 ubiquitin ligase complex that targets Mre11 for proteasome-dependent degradation (4, 55, 87, 111, 133). Since viral DNA replication is inhibited if MRN is not inactivated, one would anticipate that inhibition of the MRN complex would need to occur prior to the onset of viral DNA replication for both E4-induced mechanisms of MRN inactivation. This prediction holds true for E4-ORF3, but it was not apparent if this applied to MRN degradation induced by E1B-55K–E4-ORF6 since significant levels of MRN were evident at times of viral DNA replication (87, 133). If this did not take place, it would suggest either a new mechanism of MRN inhibition or may lead to insight into the initial recognition of the viral genome by the MRN complex.

The MRN complex is degraded in an E4-ORF6/E1B-55K-dependent manner before viral DNA accumulation.

The results of biochemical analyses on infected cell populations indicated that very little MRN degradation was evident at the onset of viral DNA replication. In cells infected with a virus mutant that lacks E4-ORF3 (inORF3), MRN protein levels were only reduced ~two-fold at the onset of viral DNA replication (Figs. 1 and 2). Significant MRN degradation was not seen until 14-18 hpi when the viral genome had been amplified >100-fold. This suggested that there were significant levels of the MRN complex still present in the cell by the time viral DNA replication was occurring. Another mechanism employed by the virus to inhibit the MRN complex is relocalization. Mre11 is transported to the cytoplasm where it eventually

forms aggresomes that are thought to increase the efficiency of proteasomal-dependent degradation and can inhibit DNA damage foci formation (4, 87). These aggresomes are not seen until late times during infection and I did not find any aggresomes in our immunofluorescence assays at 8 hpi, however, proteins will generally aggregate in the cytoplasm and then move along microtubules to the MTOC (microtubule organizing center) to form an aggresome (49). If the early inhibition of the MRN complex were due to a relocalization to the cytoplasm that preceded aggresome formation, the fractionation experiment should have shown an increase in cytoplasmic accumulation of the components of the MRN complex. The majority of MRN was localized to the nucleus in these assays (Fig. 3), suggesting the inhibition of the MRN complex was not due to relocalization.

The DSBR-induced checkpoint signaling is inactivated by the time viral DNA replication occurs.

These results appear to be contradicted by single cell assays which showed that a checkpoint signaling response, the phosphorylation of ATM which is dependent on MRN activity, was inhibited by E1B-55K–E4-ORF6 by the time viral DNA accumulation occurred (Figs. 9, 10). This applied to checkpoint signaling induced by Ad genomes delivered by the initial infection as well as checkpoint signaling induced by DNA damage. Further, single cell immunofluorescence assays indicated degradation of the MRN complex in infected cells staining positive for DBP prior to viral DNA accumulation (Figs. 4-8). The reduction in MRN levels was dependent on E1B-55K and E4-ORF6 and required a CUL5-containing E3 ubiquitin ligase complex (Figs. 7, 8). Corbin-Lickfett and Bridge have shown that active proteasomes are not necessary after 8 hpi for E1B-55K–E4-ORF6-dependent promotion of late gene expression (31). This is consistent with the findings presented here in that the E1B-55K–E4-ORF6 ubiquitin ligase activity functions early during infection to degrade the MRN complex.

The discrepancy observed between these analyses can be explained by noting the difference between the population-based and single-cell-based

assays. At 8 hpi, only about half of the cells express DBP to levels visible by immunofluorescence. When stained at 18 hpi, after infecting with the same multiplicity of infection, nearly all the cells are DBP positive (data not shown). This suggests that within a population of infected cells, the infections proceed at different rates. Two contributing factors in the rate of progression may depend on the varying amounts of viral genomes that will enter the nucleus of each cell--the presence of more genomes may accelerate the viral life cycle. Also, in an unsynchronized population of cells, those cells already in S phase may proceed through the viral life cycle more quickly (52, 124). For these reasons, I believe that the two-fold decrease in Mre11 levels detected by Western blot at 10 hpi (Fig. 1) is due to a nearly complete loss of Mre11 in about half of the cells rather than a loss of half of the Mre11 in all of the cells. Under these assumptions, it would follow that viral DNA replication is occurring earlier in some cells and that this would coordinate with those cells expressing higher levels of DBP. To this end, I can conclude that when cells are replicating viral DNA, they are expressing higher levels of DBP, the MRN complex has been degraded, and checkpoint signaling is inhibited even when newly introduced double-stranded breaks are present. While I cannot show conclusively when the first rounds of replication are occurring, it seems likely that MRN degradation is complete, or at least nearly complete, prior to the onset of viral DNA replication. Finally, I conclude from the pATM assays (Fig. 9) that input Ad genomes from the initial viral infection are sufficient to be recognized by the MRN complex and induce a DSBR response. The latter conclusion is consistent with results indicating that Ad infection leads to the formation of Mdc1 foci early after infection (94).

Terminal protein is not cleaved from the genomes in double mutant infections at a time when checkpoint signaling is occurring.

Since Mre11 has nucleolytic activity and the ends of the Ad genome will need to be processed at the least to remove the covalently-attached TP, in order to be ligated together, I examined the integrity of the termini of the Ad genome at 10 hpi under conditions where MRN was, or was not, inactivated.

These results (Fig. 11) showed that there was no cleavage of TP from wild type, single mutant, or double mutant genomes. This suggests that the MRN complex does not induce endonucleolytic degradation of the Ad genome by 10 hpi, even though there are pATM foci forming, indicative of sites of DNA damage repair. I also did not see any evidence for concatemer junction formation at this time point since the levels of the terminal restriction fragments in double mutant virus infections corresponded equally to internal fragments—a reduction in the levels of terminal fragments should be observed relative to internal fragments if significant concatenation occurred. It is possible that large concatemeric Ad DNAs were excluded from isolation using the Hirt extraction procedure (57) that I used to isolate viral DNA. However, our results are entirely consistent with those of Weiden and Ginsberg where Ad genome concatenation was found at late, but not early times after infection (152). Also, our results are consistent with the recent finding from Lakdawala *et al*. that show that concatenation does not cause the viral DNA replication inhibition (77).

There have been several hypotheses over the years as to the exact mechanism of inhibition. One idea was that concatenation of the genomes disrupted the origins of replication and prevented efficient viral DNA replication. Since concatenation does not appear to occur prior to viral DNA replication during an infection, it seems like an unlikely cause of inhibition. Also, it was recently shown not to be the case using MO59J cells, which lack DNA-PK and do not allow for concatenation (77). In these cells, viral DNA replication was not rescued and this defect was still seen without concatenation. Another aspect of DSBR that may have served a role in the inhibition of viral DNA replication was the checkpoint signaling response elicited through ATM. This also seems irrelevant to viral DNA replication in that replication was not rescued in A-T cells, which lack a functional ATM (77). A-T cells were also treated with caffeine to inhibit ATR, the other PIKK that may be able to compensate for ATM. Under these conditions, viral DNA replication was still inhibited suggesting that the checkpoint signaling

response is not necessary to inhibit replication (77). A third mechanism of inhibition proposed is that the nucleolytic activity of Mre11 can degrade the ends of the viral genome and that this will destroy the origins of replication. Even the degradation of a few nucleotides can theoretically inhibit replication due to the replication mechanism. It involves a jumping back process that places the initial cytosine, covalently linked to pTP at the fourth nucleotide before it jumps back to nucleotide one (122). The nuclease activity of Mre11 is necessary for downstream effects, such as concatenation (133), but its effect on viral DNA replication has not been determined. The results from the TP cleavage assay suggest that it is not important, as the endonucleolytic activity had not caused the cleavage of TP at a time when viral DNA replication would have been inhibited. The junctions of the concatemers have been sequenced and it was revealed that the deletions made are rather large, ranging from ~500bp to 5kb (69). Degradation of that extent, even if only of the 3' strand from the exonucleolytic activity of Mre11, would have been detected in the proteinase K-treated samples of the TP cleavage assay.

Protection of the incoming genome from the DSBR response.

The results of the TP cleavage assay also provided evidence to suggest another hypothesis pertaining to a different aspect of adenoviral infection was false. The MRN complex will recognize the Ad genome and elicit a DSBR response if the viral proteins that inhibit the MRN complex (E4-ORF3, E4-ORF6, and E1B-55K) are not expressed. During wild type infections, however, these viral proteins are not expressed to significant levels until several hours after the incoming genomes reach the nucleus, yet there are no detrimental effects of the MRN complex on the Ad genome until, or after, viral DNA replication is initiated, suggesting that the incoming genomes are protected from MRN recognition during the earliest stages of infection. It has been hypothesized that the Ad TP can protect the incoming genomes from recognition by the MRN complex and that eventually, MRN will cleave the termini in a similar fashion to the way it cleaves Spo11 from meiotic-specific DSBs in *S.cerevisiae* (133, 154). Since this is not the case, it may be

that there is some other unknown mechanism to mask the viral genome and protect it from MRN recognition or the detrimental effects that occur following MRN induction of a DSBR response. When the pATM foci that form during a double mutant infection were visualized in relation to viral genomes, an unexpected result hinted at another explanation.

While doing immunofluorescence assays to further study the pATM foci that form in response to a double mutant infection, I fully expected that these foci represented checkpoint signaling occurring at viral genomes. It was surprising to find that the pATM foci and VII dots, which represent viral genomes, did not colocalize, but led us to the idea that mutually exclusive binding could be representative of the elusive protective factor that I had shown not to be TP. If VII acted to protect the viral genome from MRN recognition early during infection, then it would make sense that the two proteins did not colocalize, but still allowed for the possibility that the pATM foci have formed at viral genomes. Instead of using a protein marker of viral DNA, I utilized the Click-iT Edu imaging kit to label the DNA directly and found that both the VII dots as well as the pATM foci colocalized with viral DNA (Fig. 12). It also stands to reason then, that γH2AX foci are forming at viral genomes since they colocalize with pATM as well during a double mutant infection (Fig. 12). How or when these histones bind to viral DNA, or if they are accompanied by other histones is not known, but is in itself a novel discovery.

Chen *et al.* discovered that VII remains on the genome during the initial phase of infection and is only released after higher levels of transcription occur around 10-12 hpi (29). This happens to coincide with the time during infection when checkpoint signaling is occurring. To visualize the loss of VII alongside the formation of pATM foci, a time course was performed in which the number of foci of both VII and pATM were quantitated (Fig. 13). At 6 hpi, VII dots begin to decrease as pATM foci increase at an inverse rate. Also, throughout the time course, the total amount of foci, be it protein VII or pATM, remained the same throughout (Fig. 14). Together, these results suggest that

there is mutually exclusive binding, which may indicate that one protein, viral protein VII, has the ability to prevent the other protein, pATM, and MRN by extension, from binding viral DNA. It was also determined that the inhibition of transcription, but not DNA replication, inhibited pATM foci formation as well as the release of VII from the viral genomes (Fig. 15). This further suggests that the release of VII is connected to checkpoint signaling since they are both initiated by transcription. While this result does not show that it is VII release itself and not a coincidental reliance on transcription, it fits a model in which VII can protect the genome from recognition by the MRN complex, but once released, MRN can recognize the dsDNA viral genome and elicit a checkpoint signaling response. Even still, I cannot rule out the possibility that it is transcription itself that somehow alerts the MRN complex to the viral genome or transcription of an early gene that plays a role in eliciting a checkpoint signaling response.

Mechanism of inhibition of viral DNA replication.

There is still the open-ended question of how the inhibition of viral DNA replication occurs in E4-deleted virus infections since the nuclease activity of Mre11 does not appear to be the mechanism. When looking back at the results from the replication assay, it supports the data that show that degradation of the viral termini is not causing the inhibition. As expected, viral DNA accumulation was significantly delayed for the double mutant that lacks both E4-ORF3 and E4-ORF6 (dl355/inORF3), however at 15 hpi, the viral DNA began accumulating at a similar rate to wild type (Fig. 2) as shown previously in an Ad2 E4 mutant by Yoder and Berget (162). This suggests that one of the following is true. The inhibition of viral DNA replication due to the activity of the MRN complex is reversible, that it is not complete, and there is a threshold effect whereby some genomes escape MRN activity, or the E4 proteins have an additional, unknown function that accelerates viral DNA replication and that the inhibition seen is merely a delay due to the absence of stimulatory factors. In either case, degradation of the termini should be a

permanent effect and would not account for the replication seen at late times during infection.

The replication assay performed here stopped at 24 hpi and did not determine if viral DNA levels of E4-mutated virus infections will eventually reach wild type, which would raise the issue of what else is contributing to the low virus yield since it does not reach wild type levels. Even if viral DNA replication reaches wild type levels, late gene transcription also is reduced in E4-deleted infections (54, 153, 162) and could account for the low virus yield. Our replication assay would not discriminate between monomeric and concatemeric viral genomes. A large portion of those genomes are most likely part of a concatemeric molecule, which would prevent packaging, as it is too large, and would effect virus yield. There is also evidence to suggest that concatemeric genomes are not efficient templates for late gene transcription (64).

I propose a model in which simply the presence of the MRN complex on the viral termini will prevent the formation of the pre-initiation complexes necessary for viral DNA replication (Fig. 16). The idea is that VII will remain on the viral genomes as they enter the nucleus and prevent recognition by the MRN complex. Early transcription will occur at relatively low levels, possibly due to the transcriptionally repressive activity of VII. Early proteins will eventually accumulate and the E4 proteins will inhibit the MRN complex, at which point, higher levels of transcription are induced to release VII from the genome. The E2 proteins, which include the viral proteins necessary for viral DNA replication, will also accumulate and form pre-initiation complexes (PICs) to initiate replication. In an E4-deleted virus, once VII is released from the genome, the MRN complex can form checkpoint signaling foci at the termini of the genomes. It seems possible that there might be competition between PIC formation and MRN binding since they occur at the same time during infection with an E4-deleted virus and occupy the same regions on the viral genome. In this way, the presence of the MRN complex would prevent PIC formation and inhibit viral DNA replication, however, if PIC formation

Figure 16.

Competition model. The viral genome will enter the nucleus bound by protein VII. With higher levels of transcription at around 6 hpi, VII is released. Without inhibition of the MRN complex by the E4 proteins, there is competition between checkpoint signaling foci formation at the genomic termini and pre-initiation complex formation at the origins of replication. This competition prevents efficient viral DNA replication, but can be rescued by a decrease in the amount of available MRN complex.

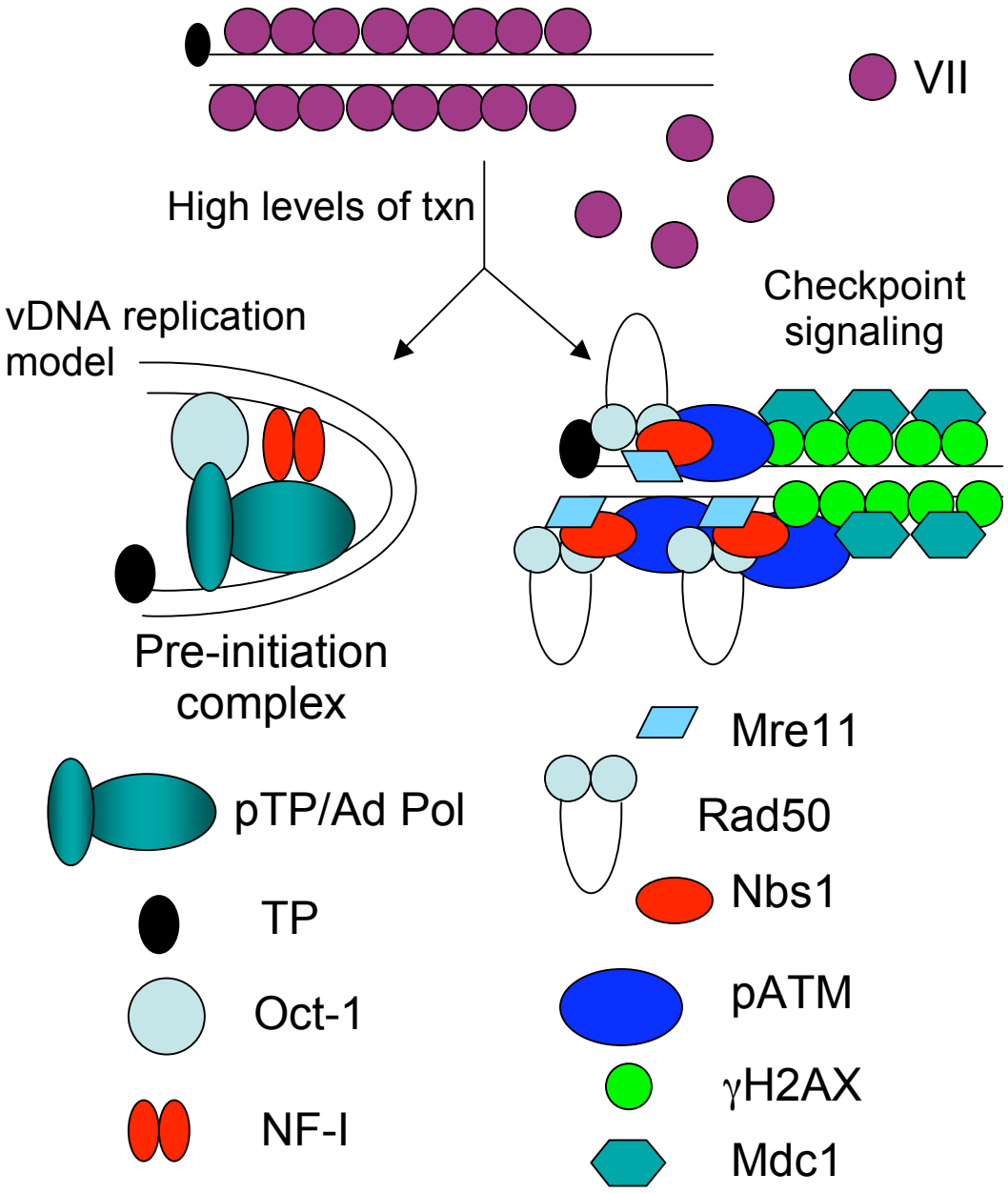

occurs prior to MRN recognition on a portion of viral genomes within one cell, replication of that genome will ensue. As long as there is a low level of replication occurring within the cell, as the infection progresses, more and more of the MRN complex will be titrated out by binding to susceptible viral genomes and more E2 proteins will be produced making it increasingly more likely for PIC formation to occur rather than MRN binding. The ratio of E2 proteins to available MRN complexes would eventually surpass the threshold upon which viral DNA replication would begin to occur at a rate near wild type levels as seen by the replication assay.

The competition model raises more questions about how much of the checkpoint signaling foci are necessary to preclude PIC formation. Since the checkpoint signaling foci that form are very large and cover an extensive region of the DNA beginning at the very terminus of the broken strand, it is easy to imagine how this would interfere with PIC formation. However, the evidence from the studies done by Lakdawala *et al*. suggest that if the model is accurate, it is MRN alone that must be able to inhibit PIC formation seeing as ATM or ATR are not required for the replication block, but are necessary to elicit the checkpoint signaling response that initiates the formation of the large IRIF (77). One must then question if the MRN complex is large enough or can bind in a way to prevent efficient binding of PIC proteins. The crystal structure of the M_2R_2 heterotetramer bound to DNA (157) suggests that it is reasonable to think that the MRN complex can mask at least the very terminus of the DNA, which would prevent pTP from being able to bind to the fourth nucleotide and initiate the priming reaction of viral DNA replication.

While the idea that viral protein VII can prevent the large checkpoint signaling foci from forming is very plausible since they would be occupying the same space on the viral genome, preventing even the initial recognition of the viral genome by the MRN complex is slightly harder to accept. The exact structure of viral chromatin with protein VII is not known. It is spread over the entire genome, but whether it is present in significant quantities at the termini remains to be seen. If not, it is unknown how VII could prevent MRN binding,

but it would have to since MRN alone has such a significant effect on viral DNA replication. One possibility is that the VII/genome structure is somehow able to prevent a more stable binding of MRN that would thus allow for PIC formation to compete with MRN for the genomic termini. Another possibility is that VII does bind to the termini and the structure is such that it prevents MRN binding altogether. Another interesting point to take into consideration is that the MRN complex can recognize and bind to DSBs within cellular chromatin. It seems possible that the introduction of a DSB disrupts the organized structure that the histones create with cellular DNA and that this could allow the DSBs to be more available for MRN binding while the viral genome is in a stable, linear structure. Also, chromatin remodeling seems to play a role in DSBR and while it is independent of ATM and H2AX, it requires the MRN complex and ATP, suggesting it is more than simply relief of torsional stress established during the packaging of chromatin (76, 146). The local chromatin expansion of the cellular histones may not come into play with the viral genome. It may be this reorganization of cellular chromatin that allows for MRN binding at DSBs that the virus may have selected against for its chromatin structure with VII, throughout its evolution, to prevent MRN from recognizing the viral genomes and thus, allowing PIC formation.

Another possibility is that VII-bound viral DNA may resemble heterochromatic regions while the release of VII creates a viral genomic structure that is similar to euchromatic regions, at least in their response to DSBs. Studies have shown that γH2AX foci form preferentially at regions of euchromatin, and that there are islands within a nucleus that lack γH2AX foci and correspond to regions of heterochromatin as seen by HP1α staining, a conserved marker of heterochromatic regions (33). In this way, VII would act to compact the viral DNA into a structure that prevents MRN recognition as seen with DSBs in cellular heterochromatin.

Here I have studied the importance of inhibiting the MRN complex in terms of Ad viral DNA replication. I show that the inhibition of the MRN complex precedes viral DNA replication and that the block at replication does

not appear to be due to Mre11 nucleolytic degradation of the genomic termini and therefore, the origins of replication, but the presence of the MRN complex itself. I propose that viral protein VII can hold the MRN complex off while bound to the viral DNA, and that once released, there exists competition between the replication machinery forming the PIC on the origins of replication and the MRN complex forming checkpoint signaling foci on the genomic termini that are perceived as DSBs. The ability of VII to protect the viral genome from MRN recognition during the initial phase of infection is a novel function of this protein. Exploring Ad viral DNA replication has served as an important way to study the DSBR pathway, particularly the MRN complex.

Future Directions

The competition model I proposed still has several areas left to explore. First, clarifying the role of the exonucleolytic activity of Mre11 can be determined. While endonucleolytic digestion of the viral genome did not occur by 10 hpi in an E4-ORF3/E4-ORF6 mutant infection, the resolution of the TP cleavage assay is not high enough to rule out minimal exonucleolytic digestion of the 3' strand. To determine if the nucleolytic activity of Mre11 plays a role in inhibiting viral DNA replication, the nuclease-defective Mre11 mutant, Mre11-3, can be utilized (5). Mre11-3 retains the ability to bind DNA as well as Rad50 and Nbs1, but the mutation disrupts the nucleolytic activity. Mutant viruses were constructed using dl366 (E4-deleted) as a backbone with wild type or mutant Mre11 expressed from the CMV promoter in place of the E1 genes (constructed by Dr. Patrick Hearing). These viruses can be used to infect ATLD1 cells, which have a hypomorphic mutation in Mre11, and have been immortalized by transduction with retroviruses expressing SV40 T-antigen and hTERT (gift from Dr. Matthew Weitzman). Viral DNA can be isolated at 30 hpi to analyze newly replicated viral DNA and at 4 hpi for comparison to input viral DNA. Quantitative PCR (qPCR) can then be used to analyze the amount of viral DNA replication under the different conditions. Infection of ATLD1 cells with dl366 should rescue for viral DNA replication since there is no Mre11, however, co-infections of parental dl366 with dl366 expressing wild type Mre11, should restore MRN function and prevent efficient replication. Co-infection of dl366 with dl366 expressing Mre11-3 will show whether the nuclease activity of Mre11 is important for inhibiting viral DNA replication. If replication ensues, this would suggest that the cause of the inhibition is due to the exonuclease activity, while poor replication would show that the nuclease activity of Mre11 is not necessary to inhibit viral DNA replication.

Another aspect to explore is the delay of viral DNA replication seen with E4-deleted viruses. I proposed that the cause of the increased level of replication later during infection is due to the weakening of the competition

between PIC formation and MRN complex recognition due to titration of the MRN complex. By analyzing the timing of viral DNA replication in A-T cells, I may gain clues as to whether this is an accurate model. A-T cells have non-functional, mutated ATM, which should prevent formation of the large checkpoint signaling foci that would normally form on DSBs, as well as viral genomes. First, immunofluorescence of these cells following infection with dl355/inORF3 should be done to ensure that there is no γH2AX or Mdc1 foci forming at the viral genomes. Next, viral DNA replication can be analyzed by qPCR, similarly to the Mre11-3 experiment. If replication is even more delayed, this would suggest that since MRN is not forming larger checkpoint signaling foci and thus, not be titrated out as efficiently, that it will take longer for PIC formation to out-compete MRN recognition. Since viral DNA replication is delayed in A-T cells even with wild type virus, a control of A-T cells expressing ATM should be used (108). Alternatively, RNAi knockdown of ATM could be performed.

The mutually exclusive binding between VII and pATM can also be explored further. ChIP–reChIP (sequential chromatin immunoprecipitation) experiments can be done using sequential immunoprecipitation (IP) of VII, then pATM, and vice versa. The viral DNA that is pulled down at the end of each step can be analyzed by qPCR to determine if both proteins ever bind the viral genome at the same time. Similarly, ChIP–reChIP can be used to determine if both pATM and Ad polymerase (Ad pol) can bind to the viral genome at the same time. This would determine if the PIC could form on viral DNA that is bound by pATM and the rest of the checkpoint signaling proteins. Finally, another ChIP experiment to perform would be to do an IP with antibodies to different histones, particularly H2AX, and follow it up with qPCR of different regions of the viral genome. The presence of histones on Ad genomes is not known. Immunofluoresence assays have shown that γH2AX foci do form at what can be presumed to be checkpoint signaling foci on the viral genomes. How extensive the coverage is remains to be seen as well as

if there are any other histones present on viral DNA. Also, this has only been seen with dl355/in, so studies involving wild type Ad would be useful as well.

References

1. **Alestrom, P., G. Akusjarvi, M. Lager, L. Yeh-kai, and U. Pettersson.** 1984. Genes encoding the core proteins of adenovirus type 2. J Biol Chem **259:**13980-5.
2. **Amin, M., A. Mirza, and J. Weber.** 1977. Genetic analysis of adenovirus type 2. VII. Cleavage-modified affinity for DNA of internal virion proteins. Virology **80:**83-97.
3. **Anderson, C. W., M. E. Young, and S. J. Flint.** 1989. Characterization of the adenovirus 2 virion protein, mu. Virology **172:**506-12.
4. **Araujo, F. D., T. H. Stracker, C. T. Carson, D. V. Lee, and M. D. Weitzman.** 2005. Adenovirus type 5 E4orf3 protein targets the Mre11 complex to cytoplasmic aggresomes. J Virol **79:**11382-91.
5. **Arthur, L. M., K. Gustausson, K. P. Hopfner, C. T. Carson, T. H. Stracker, A. Karcher, D. Felton, M. D. Weitzman, J. Tainer, and J. P. Carney.** 2004. Structural and functional analysis of Mre11-3. Nucleic Acids Res **32:**1886-93.
6. **Ascoli, C. A., and G. G. Maul.** 1991. Identification of a novel nuclear domain. J Cell Biol **112:**785-95.
7. **Baker, A., K. J. Rohleder, L. A. Hanakahi, and G. Ketner.** 2007. Adenovirus E4 34k and E1b 55k oncoproteins target host DNA ligase IV for proteasomal degradation. J Virol **81:**7034-40.
8. **Bakkenist, C. J., and M. B. Kastan.** 2003. DNA damage activates ATM through intermolecular autophosphorylation and dimer dissociation. Nature **421:**499-506.
9. **Barker, D. D., and A. J. Berk.** 1987. Adenovirus proteins from both E1B reading frames are required for transformation of rodent cells by viral infection and DNA transfection. Virology **156:**107-21.
10. **Berget, S. M., C. Moore, and P. A. Sharp.** 1977. Spliced segments at the 5' terminus of adenovirus 2 late mRNA. Proc Natl Acad Sci U S A **74:**3171-5.
11. **Berk, A. J., F. Lee, T. Harrison, J. Williams, and P. A. Sharp.** 1979. Pre-early adenovirus 5 gene product regulates synthesis of early viral messenger RNAs. Cell **17:**935-44.
12. **Bhaskara, V., A. Dupre, B. Lengsfeld, B. B. Hopkins, A. Chan, J. H. Lee, X. Zhang, J. Gautier, V. Zakian, and T. T. Paull.** 2007. Rad50 adenylate kinase activity regulates DNA tethering by Mre11/Rad50 complexes. Mol Cell **25:**647-61.
13. **Boisvert, F. M., M. J. Hendzel, and D. P. Bazett-Jones.** 2000. Promyelocytic leukemia (PML) nuclear bodies are protein structures that do not accumulate RNA. J Cell Biol **148:**283-92.
14. **Borden, K. L.** 2002. Pondering the promyelocytic leukemia protein (PML) puzzle: possible functions for PML nuclear bodies. Mol Cell Biol **22:**5259-69.
15. **Boyer, J., K. Rohleder, and G. Ketner.** 1999. Adenovirus E4 34k and E4 11k inhibit double strand break repair and are physically associated with the cellular DNA-dependent protein kinase. Virology **263:**307-12.

16. **Bridge, E., and G. Ketner.** 1989. Redundant control of adenovirus late gene expression by early region 4. J Virol **63:**631-8.
17. **Brown, D. T., M. Westphal, B. T. Burlingham, U. Winterhoff, and W. Doerfler.** 1975. Structure and composition of the adenovirus type 2 core. J Virol **16:**366-87.
18. **Burma, S., B. P. Chen, M. Murphy, A. Kurimasa, and D. J. Chen.** 2001. ATM phosphorylates histone H2AX in response to DNA double-strand breaks. J Biol Chem **276:**42462-7.
19. **Campbell, E. M., and T. J. Hope.** 2005. Gene therapy progress and prospects: viral trafficking during infection. Gene Ther **12:**1353-9.
20. **Carson, C. T., R. A. Schwartz, T. H. Stracker, C. E. Lilley, D. V. Lee, and M. D. Weitzman.** 2003. The Mre11 complex is required for ATM activation and the G2/M checkpoint. Embo J **22:**6610-20.
21. **Casavant, N. C., M. H. Luo, K. Rosenke, T. Winegardner, A. Zurawska, and E. A. Fortunato.** 2006. Potential role for p53 in the permissive life cycle of human cytomegalovirus. J Virol **80:**8390-401.
22. **Celeste, A., O. Fernandez-Capetillo, M. J. Kruhlak, D. R. Pilch, D. W. Staudt, A. Lee, R. F. Bonner, W. M. Bonner, and A. Nussenzweig.** 2003. Histone H2AX phosphorylation is dispensable for the initial recognition of DNA breaks. Nat Cell Biol **5:**675-9.
23. **Celeste, A., S. Petersen, P. J. Romanienko, O. Fernandez-Capetillo, H. T. Chen, O. A. Sedelnikova, B. Reina-San-Martin, V. Coppola, E. Meffre, M. J. Difilippantonio, C. Redon, D. R. Pilch, A. Olaru, M. Eckhaus, R. D. Camerini-Otero, L. Tessarollo, F. Livak, K. Manova, W. M. Bonner, M. C. Nussenzweig, and A. Nussenzweig.** 2002. Genomic instability in mice lacking histone H2AX. Science **296:**922-7.
24. **Cerosaletti, K., and P. Concannon.** 2004. Independent roles for nibrin and Mre11-Rad50 in the activation and function of Atm. J Biol Chem **279:**38813-9.
25. **Cerosaletti, K., J. Wright, and P. Concannon.** 2006. Active role for nibrin in the kinetics of atm activation. Mol Cell Biol **26:**1691-9.
26. **Challberg, M. D., S. V. Desiderio, and T. J. Kelly, Jr.** 1980. Adenovirus DNA replication in vitro: characterization of a protein covalently linked to nascent DNA strands. Proc Natl Acad Sci U S A **77:**5105-9.
27. **Chapman, J. R., and S. P. Jackson.** 2008. Phospho-dependent interactions between NBS1 and MDC1 mediate chromatin retention of the MRN complex at sites of DNA damage. EMBO Rep **9:**795-801.
28. **Chatterjee, P. K., M. E. Vayda, and S. J. Flint.** 1985. Interactions among the three adenovirus core proteins. J Virol **55:**379-86.
29. **Chen, J., N. Morral, and D. A. Engel.** 2007. Transcription releases protein VII from adenovirus chromatin. Virology **369:**411-22.
30. **Clatworthy, A. E., M. A. Valencia-Burton, J. E. Haber, and M. A. Oettinger.** 2005. The MRE11-RAD50-XRS2 complex, in addition to other non-homologous end-joining factors, is required for V(D)J joining in yeast. J Biol Chem **280:**20247-52.

31. **Corbin-Lickfett, K. A., and E. Bridge.** 2003. Adenovirus E4-34kDa requires active proteasomes to promote late gene expression. Virology **315:**234-44.
32. **Cortez, D., S. Guntuku, J. Qin, and S. J. Elledge.** 2001. ATR and ATRIP: partners in checkpoint signaling. Science **294:**1713-6.
33. **Cowell, I. G., N. J. Sunter, P. B. Singh, C. A. Austin, B. W. Durkacz, and M. J. Tilby.** 2007. gammaH2AX foci form preferentially in euchromatin after ionising-radiation. PLoS One **2:**e1057.
34. **D'Amours, D., and S. P. Jackson.** 2002. The Mre11 complex: at the crossroads of dna repair and checkpoint signalling. Nat Rev Mol Cell Biol **3:**317-27.
35. **Daikoku, T., A. Kudoh, Y. Sugaya, S. Iwahori, N. Shirata, H. Isomura, and T. Tsurumi.** 2006. Postreplicative mismatch repair factors are recruited to Epstein-Barr virus replication compartments. J Biol Chem **281:**11422-30.
36. **Dallaire, F., P. Blanchette, P. Groitl, T. Dobner, and P. E. Branton.** 2009. Identification of integrin alpha3 as a new substrate of the adenovirus E4orf6/E1B 55-kilodalton E3 ubiquitin ligase complex. J Virol **83:**5329-38.
37. **de Jager, M., M. L. Dronkert, M. Modesti, C. E. Beerens, R. Kanaar, and D. C. van Gent.** 2001. DNA-binding and strand-annealing activities of human Mre11: implications for its roles in DNA double-strand break repair pathways. Nucleic Acids Res **29:**1317-25.
38. **de Jager, M., C. Wyman, D. C. van Gent, and R. Kanaar.** 2002. DNA end-binding specificity of human Rad50/Mre11 is influenced by ATP. Nucleic Acids Res **30:**4425-31.
39. **Desai-Mehta, A., K. M. Cerosaletti, and P. Concannon.** 2001. Distinct functional domains of nibrin mediate Mre11 binding, focus formation, and nuclear localization. Mol Cell Biol **21:**2184-91.
40. **di Masi, A., M. Viganotti, F. Polticelli, P. Ascenzi, C. Tanzarella, and A. Antoccia.** 2008. The R215W mutation in NBS1 impairs gamma-H2AX binding and affects DNA repair: molecular bases for the severe phenotype of 657del5/R215W Nijmegen breakage syndrome patients. Biochem Biophys Res Commun **369:**835-40.
41. **Digweed, M., A. Reis, and K. Sperling.** 1999. Nijmegen breakage syndrome: consequences of defective DNA double strand break repair. Bioessays **21:**649-56.
42. **Durocher, D., and S. P. Jackson.** 2001. DNA-PK, ATM and ATR as sensors of DNA damage: variations on a theme? Curr Opin Cell Biol **13:**225-31.
43. **Evans, J. D., and P. Hearing.** 2002. Adenovirus Replication, p. 39-70. *In* D. Curiel and J. Douglas (ed.), Adenoviral Vectors For Gene Therapy. Elsevier Science.
44. **Evans, J. D., and P. Hearing.** 2003. Distinct roles of the Adenovirus E4 ORF3 protein in viral DNA replication and inhibition of genome concatenation. J Virol **77:**5295-304.
45. **Evans, J. D., and P. Hearing.** 2005. Relocalization of the Mre11-Rad50-Nbs1 complex by the adenovirus E4 ORF3 protein is required for viral replication. J Virol **79:**6207-15.

46. **Everett, R. D.** 2001. DNA viruses and viral proteins that interact with PML nuclear bodies. Oncogene **20:**7266-73.
47. **Everett, R. D., and J. Murray.** 2005. ND10 components relocate to sites associated with herpes simplex virus type 1 nucleoprotein complexes during virus infection. J Virol **79:**5078-89.
48. **Furuse, M., Y. Nagase, H. Tsubouchi, K. Murakami-Murofushi, T. Shibata, and K. Ohta.** 1998. Distinct roles of two separable in vitro activities of yeast Mre11 in mitotic and meiotic recombination. Embo J **17:**6412-25.
49. **Garcia-Mata, R., Y. S. Gao, and E. Sztul.** 2002. Hassles with taking out the garbage: aggravating aggresomes. Traffic **3:**388-96.
50. **Gatei, M., D. Young, K. M. Cerosaletti, A. Desai-Mehta, K. Spring, S. Kozlov, M. F. Lavin, R. A. Gatti, P. Concannon, and K. Khanna.** 2000. ATM-dependent phosphorylation of nibrin in response to radiation exposure. Nat Genet **25:**115-9.
51. **Goldberg, M., M. Stucki, J. Falck, D. D'Amours, D. Rahman, D. Pappin, J. Bartek, and S. P. Jackson.** 2003. MDC1 is required for the intra-S-phase DNA damage checkpoint. Nature **421:**952-6.
52. **Goodrum, F. D., and D. A. Ornelles.** 1997. The early region 1B 55-kilodalton oncoprotein of adenovirus relieves growth restrictions imposed on viral replication by the cell cycle. J Virol **71:**548-61.
53. **Graham, F. L., J. Smiley, W. C. Russell, and R. Nairn.** 1977. Characteristics of a human cell line transformed by DNA from human adenovirus type 5. J Gen Virol **36:**59-74.
54. **Halbert, D. N., J. R. Cutt, and T. Shenk.** 1985. Adenovirus early region 4 encodes functions required for efficient DNA replication, late gene expression, and host cell shutoff. J Virol **56:**250-7.
55. **Harada, J. N., A. Shevchenko, A. Shevchenko, D. C. Pallas, and A. J. Berk.** 2002. Analysis of the adenovirus E1B-55K-anchored proteome reveals its link to ubiquitination machinery. J Virol **76:**9194-206.
56. **Haruki, H., M. Okuwaki, M. Miyagishi, K. Taira, and K. Nagata.** 2006. Involvement of template-activating factor I/SET in transcription of adenovirus early genes as a positive-acting factor. J Virol **80:**794-801.
57. **Hirt, B.** 1967. Selective extraction of polyoma DNA from infected mouse cell cultures. J Mol Biol **26:**365-9.
58. **Hopfner, K. P., A. Karcher, D. S. Shin, L. Craig, L. M. Arthur, J. P. Carney, and J. A. Tainer.** 2000. Structural biology of Rad50 ATPase: ATP-driven conformational control in DNA double-strand break repair and the ABC-ATPase superfamily. Cell **101:**789-800.
59. **Hosokawa, K., and M. T. Sung.** 1976. Isolation and characterization of an extremely basic protein from adenovirus type 5. J Virol **17:**924-34.
60. **Huang, M. M., and P. Hearing.** 1989. Adenovirus early region 4 encodes two gene products with redundant effects in lytic infection. J Virol **63:**2605-15.
61. **Ishov, A. M., and G. G. Maul.** 1996. The periphery of nuclear domain 10 (ND10) as site of DNA virus deposition. J Cell Biol **134:**815-26.

62. **Ishov, A. M., R. M. Stenberg, and G. G. Maul.** 1997. Human cytomegalovirus immediate early interaction with host nuclear structures: definition of an immediate transcript environment. J Cell Biol **138:**5-16.
63. **Jackson, S. A., and N. A. DeLuca.** 2003. Relationship of herpes simplex virus genome configuration to productive and persistent infections. Proc Natl Acad Sci U S A **100:**7871-6.
64. **Jayaram, S., and E. Bridge.** 2005. Genome concatenation contributes to the late gene expression defect of an adenovirus E4 mutant. Virology **342:**286-96.
65. **Jazayeri, A., J. Falck, C. Lukas, J. Bartek, G. C. Smith, J. Lukas, and S. P. Jackson.** 2006. ATM- and cell cycle-dependent regulation of ATR in response to DNA double-strand breaks. Nat Cell Biol **8:**37-45.
66. **Johnson, J. S., Y. N. Osheim, Y. Xue, M. R. Emanuel, P. W. Lewis, A. Bankovich, A. L. Beyer, and D. A. Engel.** 2004. Adenovirus protein VII condenses DNA, represses transcription, and associates with transcriptional activator E1A. J Virol **78:**6459-68.
67. **Jones, N., and T. Shenk.** 1979. Isolation of adenovirus type 5 host range deletion mutants defective for transformation of rat embryo cells. Cell **17:**683-9.
68. **Kamura, T., D. Burian, Q. Yan, S. L. Schmidt, W. S. Lane, E. Querido, P. E. Branton, A. Shilatifard, R. C. Conaway, and J. W. Conaway.** 2001. Muf1, a novel Elongin BC-interacting leucine-rich repeat protein that can assemble with Cul5 and Rbx1 to reconstitute a ubiquitin ligase. J Biol Chem **276:**29748-53.
69. **Karen, K. A., P. J. Hoey, C. S. Young, and P. Hearing.** 2009. Temporal regulation of the Mre11-Rad50-Nbs1 complex during adenovirus infection. J Virol **83:**4565-73.
70. **Kawai, T., and S. Akira.** 2008. Toll-like receptor and RIG-I-like receptor signaling. Ann N Y Acad Sci **1143:**1-20.
71. **Kim, J. S., T. B. Krasieva, H. Kurumizaka, D. J. Chen, A. M. Taylor, and K. Yokomori.** 2005. Independent and sequential recruitment of NHEJ and HR factors to DNA damage sites in mammalian cells. J Cell Biol **170:**341-7.
72. **Kindt, T. J., R. A. Goldsby, B. A. Osborne, and J. Kuby.** 2006. Kuby immunology. WH Freeman.
73. **Kobayashi, J., A. Antoccia, H. Tauchi, S. Matsuura, and K. Komatsu.** 2004. NBS1 and its functional role in the DNA damage response. DNA Repair (Amst) **3:**855-61.
74. **Korn, R., and M. S. Horwitz.** 1986. Adenovirus DNA synthesis in vitro is inhibited by the virus-coded major core protein. Virology **150:**342-51.
75. **Kozlov, S. V., M. E. Graham, C. Peng, P. Chen, P. J. Robinson, and M. F. Lavin.** 2006. Involvement of novel autophosphorylation sites in ATM activation. Embo J **25:**3504-14.
76. **Kruhlak, M. J., A. Celeste, G. Dellaire, O. Fernandez-Capetillo, W. G. Muller, J. G. McNally, D. P. Bazett-Jones, and A. Nussenzweig.** 2006. Changes in chromatin structure and mobility in living cells at sites of DNA double-strand breaks. J Cell Biol **172:**823-34.

77. **Lakdawala, S. S., R. A. Schwartz, K. Ferenchak, C. T. Carson, B. P. McSharry, G. W. Wilkinson, and M. D. Weitzman.** 2008. Differential requirements of the C terminus of Nbs1 in suppressing adenovirus DNA replication and promoting concatemer formation. J Virol **82:**8362-72.
78. **Lee, J. H., R. Ghirlando, V. Bhaskara, M. R. Hoffmeyer, J. Gu, and T. T. Paull.** 2003. Regulation of Mre11/Rad50 by Nbs1: effects on nucleotide-dependent DNA binding and association with ataxia-telangiectasia-like disorder mutant complexes. J Biol Chem **278:**45171-81.
79. **Lee, J. H., and T. T. Paull.** 2007. Activation and regulation of ATM kinase activity in response to DNA double-strand breaks. Oncogene **26:**7741-8.
80. **Lee, S. E., J. K. Moore, A. Holmes, K. Umezu, R. D. Kolodner, and J. E. Haber.** 1998. Saccharomyces Ku70, mre11/rad50 and RPA proteins regulate adaptation to G2/M arrest after DNA damage. Cell **94:**399-409.
81. **Leith, I. R., R. T. Hay, and W. C. Russell.** 1989. Adenovirus subviral particles and cores can support limited DNA replication. J Gen Virol **70 (Pt 12):**3235-48.
82. **Lichy, J. H., M. S. Horwitz, and J. Hurwitz.** 1981. Formation of a covalent complex between the 80,000-dalton adenovirus terminal protein and 5'-dCMP in vitro. Proc Natl Acad Sci U S A **78:**2678-82.
83. **Lilley, C. E., C. T. Carson, A. R. Muotri, F. H. Gage, and M. D. Weitzman.** 2005. DNA repair proteins affect the lifecycle of herpes simplex virus 1. Proc Natl Acad Sci U S A **102:**5844-9.
84. **Lilley, C. E., R. A. Schwartz, and M. D. Weitzman.** 2007. Using or abusing: viruses and the cellular DNA damage response. Trends Microbiol **15:**119-26.
85. **Lim, D. S., S. T. Kim, B. Xu, R. S. Maser, J. Lin, J. H. Petrini, and M. B. Kastan.** 2000. ATM phosphorylates p95/nbs1 in an S-phase checkpoint pathway. Nature **404:**613-7.
86. **Lisby, M., J. H. Barlow, R. C. Burgess, and R. Rothstein.** 2004. Choreography of the DNA damage response: spatiotemporal relationships among checkpoint and repair proteins. Cell **118:**699-713.
87. **Liu, Y., A. Shevchenko, A. Shevchenko, and A. J. Berk.** 2005. Adenovirus exploits the cellular aggresome response to accelerate inactivation of the MRN complex. J Virol **79:**14004-16.
88. **Lou, Z., K. Minter-Dykhouse, S. Franco, M. Gostissa, M. A. Rivera, A. Celeste, J. P. Manis, J. van Deursen, A. Nussenzweig, T. T. Paull, F. W. Alt, and J. Chen.** 2006. MDC1 maintains genomic stability by participating in the amplification of ATM-dependent DNA damage signals. Mol Cell **21:**187-200.
89. **Lou, Z., K. Minter-Dykhouse, X. Wu, and J. Chen.** 2003. MDC1 is coupled to activated CHK2 in mammalian DNA damage response pathways. Nature **421:**957-61.
90. **Lukas, C., F. Melander, M. Stucki, J. Falck, S. Bekker-Jensen, M. Goldberg, Y. Lerenthal, S. P. Jackson, J. Bartek, and J. Lukas.** 2004. Mdc1 couples DNA double-strand break recognition by Nbs1 with its H2AX-dependent chromatin retention. Embo J **23:**2674-83.

91. **Luo, G., M. S. Yao, C. F. Bender, M. Mills, A. R. Bladl, A. Bradley, and J. H. Petrini.** 1999. Disruption of mRad50 causes embryonic stem cell lethality, abnormal embryonic development, and sensitivity to ionizing radiation. Proc Natl Acad Sci U S A **96:**7376-81.
92. **Maizel, J. V., Jr., D. O. White, and M. D. Scharff.** 1968. The polypeptides of adenovirus. II. Soluble proteins, cores, top components and the structure of the virion. Virology **36:**126-36.
93. **Maser, R. S., K. J. Monsen, B. E. Nelms, and J. H. Petrini.** 1997. hMre11 and hRad50 nuclear foci are induced during the normal cellular response to DNA double-strand breaks. Mol Cell Biol **17:**6087-96.
94. **Mathew, S. S., and E. Bridge.** 2007. The cellular Mre11 protein interferes with adenovirus E4 mutant DNA replication. Virology **365:**346-55.
95. **Maul, G. G.** 1998. Nuclear domain 10, the site of DNA virus transcription and replication. Bioessays **20:**660-7.
96. **Maul, G. G., D. Negorev, P. Bell, and A. M. Ishov.** 2000. Review: properties and assembly mechanisms of ND10, PML bodies, or PODs. J Struct Biol **129:**278-87.
97. **McVoy, M. A., and S. P. Adler.** 1994. Human cytomegalovirus DNA replicates after early circularization by concatemer formation, and inversion occurs within the concatemer. J Virol **68:**1040-51.
98. **Medina-Kauwe, L. K.** 2003. Endocytosis of adenovirus and adenovirus capsid proteins. Adv Drug Deliv Rev **55:**1485-96.
99. **Meier, O., and U. F. Greber.** 2003. Adenovirus endocytosis. J Gene Med **5:**451-62.
100. **Melander, F., S. Bekker-Jensen, J. Falck, J. Bartek, N. Mailand, and J. Lukas.** 2008. Phosphorylation of SDT repeats in the MDC1 N terminus triggers retention of NBS1 at the DNA damage-modified chromatin. J Cell Biol **181:**213-26.
101. **Moreau, S., J. R. Ferguson, and L. S. Symington.** 1999. The nuclease activity of Mre11 is required for meiosis but not for mating type switching, end joining, or telomere maintenance. Mol Cell Biol **19:**556-66.
102. **Moreno-Herrero, F., M. de Jager, N. H. Dekker, R. Kanaar, C. Wyman, and C. Dekker.** 2005. Mesoscale conformational changes in the DNA-repair complex Rad50/Mre11/Nbs1 upon binding DNA. Nature **437:**440-3.
103. **Negorev, D., and G. G. Maul.** 2001. Cellular proteins localized at and interacting within ND10/PML nuclear bodies/PODs suggest functions of a nuclear depot. Oncogene **20:**7234-42.
104. **Parkinson, J., S. P. Lees-Miller, and R. D. Everett.** 1999. Herpes simplex virus type 1 immediate-early protein vmw110 induces the proteasome-dependent degradation of the catalytic subunit of DNA-dependent protein kinase. J Virol **73:**650-7.
105. **Paull, T. T., and M. Gellert.** 2000. A mechanistic basis for Mre11-directed DNA joining at microhomologies. Proc Natl Acad Sci U S A **97:**6409-14.
106. **Paull, T. T., and M. Gellert.** 1999. Nbs1 potentiates ATP-driven DNA unwinding and endonuclease cleavage by the Mre11/Rad50 complex. Genes Dev **13:**1276-88.

107. **Paull, T. T., and M. Gellert.** 1998. The 3' to 5' exonuclease activity of Mre 11 facilitates repair of DNA double-strand breaks. Mol Cell **1:**969-79.
108. **Peretz, S., R. Jensen, R. Baserga, and P. M. Glazer.** 2001. ATM-dependent expression of the insulin-like growth factor-I receptor in a pathway regulating radiation response. Proc Natl Acad Sci U S A **98:**1676-81.
109. **Pfuller, R., and W. Hammerschmidt.** 1996. Plasmid-like replicative intermediates of the Epstein-Barr virus lytic origin of DNA replication. J Virol **70:**3423-31.
110. **Prage, L., and U. Pettersson.** 1971. Structural proteins of adenoviruses. VII. Purification and properties of an arginine-rich core protein from adenovirus type 2 and type 3. Virology **45:**364-73.
111. **Querido, E., P. Blanchette, Q. Yan, T. Kamura, M. Morrison, D. Boivin, W. G. Kaelin, R. C. Conaway, J. W. Conaway, and P. E. Branton.** 2001. Degradation of p53 by adenovirus E4orf6 and E1B55K proteins occurs via a novel mechanism involving a Cullin-containing complex. Genes Dev **15:**3104-17.
112. **Querido, E., R. C. Marcellus, A. Lai, R. Charbonneau, J. G. Teodoro, G. Ketner, and P. E. Branton.** 1997. Regulation of p53 levels by the E1B 55-kilodalton protein and E4orf6 in adenovirus-infected cells. J Virol **71:**3788-98.
113. **Rahal, E. A., L. A. Henricksen, Y. Li, J. J. Turchi, K. S. Pawelczak, and K. Dixon.** 2008. ATM mediates repression of DNA end-degradation in an ATP-dependent manner. DNA Repair (Amst) **7:**464-75.
114. **Rekosh, D. M., W. C. Russell, A. J. Bellet, and A. J. Robinson.** 1977. Identification of a protein linked to the ends of adenovirus DNA. Cell **11:**283-95.
115. **Rogakou, E. P., C. Boon, C. Redon, and W. M. Bonner.** 1999. Megabase chromatin domains involved in DNA double-strand breaks in vivo. J Cell Biol **146:**905-16.
116. **Rogakou, E. P., D. R. Pilch, A. H. Orr, V. S. Ivanova, and W. M. Bonner.** 1998. DNA double-stranded breaks induce histone H2AX phosphorylation on serine 139. J Biol Chem **273:**5858-68.
117. **Roth, J., C. Konig, S. Wienzek, S. Weigel, S. Ristea, and M. Dobbelstein.** 1998. Inactivation of p53 but not p73 by adenovirus type 5 E1B 55-kilodalton and E4 34-kilodalton oncoproteins. J Virol **72:**8510-6.
118. **Rothkamm, K., I. Kruger, L. H. Thompson, and M. Lobrich.** 2003. Pathways of DNA double-strand break repair during the mammalian cell cycle. Mol Cell Biol **23:**5706-15.
119. **Russell, W. C., W. G. Laver, and P. J. Sanderson.** 1968. Internal components of adenovirus. Nature **219:**1127-30.
120. **Sandler, A. B., and G. Ketner.** 1989. Adenovirus early region 4 is essential for normal stability of late nuclear RNAs. J Virol **63:**624-30.
121. **Sergeant, A., M. A. Tigges, and H. J. Raskas.** 1979. Nucleosome-like structural subunits of intranuclear parental adenovirus type 2 DNA. J Virol **29:**888-98.

122. **Shenk, T.** 1996. Adenoviridae: The Viruses and Their Replication, p. 2111-2148. *In* B. N. Fields, D. M. Knipe, P. M. Howley, R. M. Chanock, T. P. Monath, J. L. Melnick, B. Roizman, and S. E. Straus (ed.), Fields Virology, Third ed. Lippincott-Raven Publishers, Philadelphia.
123. **Shepard, R. N., and D. A. Ornelles.** 2004. Diverse roles for E4orf3 at late times of infection revealed in an E1B 55-kilodalton protein mutant background. J Virol **78:**9924-35.
124. **Shepard, R. N., and D. A. Ornelles.** 2003. E4orf3 is necessary for enhanced S-phase replication of cell cycle-restricted subgroup C adenoviruses. J Virol **77:**8593-5.
125. **Shi, Y., G. E. Dodson, S. Shaikh, K. Rundell, and R. S. Tibbetts.** 2005. Ataxia-telangiectasia-mutated (ATM) is a T-antigen kinase that controls SV40 viral replication in vivo. J Biol Chem **280:**40195-200.
126. **Shiotani, B., and L. Zou.** 2009. Single-stranded DNA orchestrates an ATM-to-ATR switch at DNA breaks. Mol Cell **33:**547-58.
127. **Shroff, R., A. Arbel-Eden, D. Pilch, G. Ira, W. M. Bonner, J. H. Petrini, J. E. Haber, and M. Lichten.** 2004. Distribution and dynamics of chromatin modification induced by a defined DNA double-strand break. Curr Biol **14:**1703-11.
128. **Smart, J. E., and B. W. Stillman.** 1982. Adenovirus terminal protein precursor. Partial amino acid sequence and the site of covalent linkage to virus DNA. J Biol Chem **257:**13499-506.
129. **Sonoda, E., M. S. Sasaki, C. Morrison, Y. Yamaguchi-Iwai, M. Takata, and S. Takeda.** 1999. Sister chromatid exchanges are mediated by homologous recombination in vertebrate cells. Mol Cell Biol **19:**5166-9.
130. **Spycher, C., E. S. Miller, K. Townsend, L. Pavic, N. A. Morrice, P. Janscak, G. S. Stewart, and M. Stucki.** 2008. Constitutive phosphorylation of MDC1 physically links the MRE11-RAD50-NBS1 complex to damaged chromatin. J Cell Biol **181:**227-40.
131. **Steegenga, W. T., N. Riteco, A. G. Jochemsen, F. J. Fallaux, and J. L. Bos.** 1998. The large E1B protein together with the E4orf6 protein target p53 for active degradation in adenovirus infected cells. Oncogene **16:**349-57.
132. **Stewart, G. S., B. Wang, C. R. Bignell, A. M. Taylor, and S. J. Elledge.** 2003. MDC1 is a mediator of the mammalian DNA damage checkpoint. Nature **421:**961-6.
133. **Stracker, T. H., C. T. Carson, and M. D. Weitzman.** 2002. Adenovirus oncoproteins inactivate the Mre11-Rad50-NBS1 DNA repair complex. Nature **418:**348-52.
134. **Stracker, T. H., D. V. Lee, C. T. Carson, F. D. Araujo, D. A. Ornelles, and M. D. Weitzman.** 2005. Serotype-specific reorganization of the Mre11 complex by adenoviral E4orf3 proteins. J Virol **79:**6664-73.
135. **Stucki, M., J. A. Clapperton, D. Mohammad, M. B. Yaffe, S. J. Smerdon, and S. P. Jackson.** 2005. MDC1 directly binds phosphorylated histone H2AX to regulate cellular responses to DNA double-strand breaks. Cell **123:**1213-26.

136. **Stucki, M., and S. P. Jackson.** 2006. gammaH2AX and MDC1: anchoring the DNA-damage-response machinery to broken chromosomes. DNA Repair (Amst) **5:**534-43.
137. **Sun, Y., Y. Xu, K. Roy, and B. D. Price.** 2007. DNA damage-induced acetylation of lysine 3016 of ATM activates ATM kinase activity. Mol Cell Biol **27:**8502-9.
138. **Takaoka, A., Z. Wang, M. K. Choi, H. Yanai, H. Negishi, T. Ban, Y. Lu, M. Miyagishi, T. Kodama, K. Honda, Y. Ohba, and T. Taniguchi.** 2007. DAI (DLM-1/ZBP1) is a cytosolic DNA sensor and an activator of innate immune response. Nature **448:**501-5.
139. **Takata, M., M. S. Sasaki, E. Sonoda, C. Morrison, M. Hashimoto, H. Utsumi, Y. Yamaguchi-Iwai, A. Shinohara, and S. Takeda.** 1998. Homologous recombination and non-homologous end-joining pathways of DNA double-strand break repair have overlapping roles in the maintenance of chromosomal integrity in vertebrate cells. Embo J **17:**5497-508.
140. **Tate, V. E., and L. Philipson.** 1979. Parental adenovirus DNA accumulates in nucleosome-like structures in infected cells. Nucleic Acids Res **6:**2769-85.
141. **Tauchi, H., S. Matsuura, J. Kobayashi, S. Sakamoto, and K. Komatsu.** 2002. Nijmegen breakage syndrome gene, NBS1, and molecular links to factors for genome stability. Oncogene **21:**8967-80.
142. **Taylor, A. M., A. Groom, and P. J. Byrd.** 2004. Ataxia-telangiectasia-like disorder (ATLD)-its clinical presentation and molecular basis. DNA Repair (Amst) **3:**1219-25.
143. **Taylor, T. J., and D. M. Knipe.** 2004. Proteomics of herpes simplex virus replication compartments: association of cellular DNA replication, repair, recombination, and chromatin remodeling proteins with ICP8. J Virol **78:**5856-66.
144. **Trentin, J. J., Y. Yabe, and G. Taylor.** 1962. The quest for human cancer viruses. Science **137:**835-41.
145. **Trujillo, K. M., S. S. Yuan, E. Y. Lee, and P. Sung.** 1998. Nuclease activities in a complex of human recombination and DNA repair factors Rad50, Mre11, and p95. J Biol Chem **273:**21447-50.
146. **Tsukuda, T., A. B. Fleming, J. A. Nickoloff, and M. A. Osley.** 2005. Chromatin remodelling at a DNA double-strand break site in Saccharomyces cerevisiae. Nature **438:**379-83.
147. **Ullman, A. J., N. C. Reich, and P. Hearing.** 2007. Adenovirus E4 ORF3 protein inhibits the interferon-mediated antiviral response. J Virol **81:**4744-52.
148. **Uziel, T., Y. Lerenthal, L. Moyal, Y. Andegeko, L. Mittelman, and Y. Shiloh.** 2003. Requirement of the MRN complex for ATM activation by DNA damage. Embo J **22:**5612-21.
149. **Vayda, M. E., K. Leong, and S. J. Flint.** 1984. Transcription of adenovirus cores in vitro. Virology **139:**152-63.
150. **Vayda, M. E., A. E. Rogers, and S. J. Flint.** 1983. The structure of nucleoprotein cores released from adenovirions. Nucleic Acids Res **11:**441-60.

151. **Weber, J. M., G. Khittoo, and A. R. Bhatti.** 1983. Adenovirus core proteins. Can J Microbiol **29:**235-41.
152. **Weiden, M. D., and H. S. Ginsberg.** 1994. Deletion of the E4 region of the genome produces adenovirus DNA concatemers. Proc Natl Acad Sci U S A **91:**153-7.
153. **Weinberg, D. H., and G. Ketner.** 1986. Adenoviral early region 4 is required for efficient viral DNA replication and for late gene expression. J Virol **57:**833-8.
154. **Weitzman, M. D., and D. A. Ornelles.** 2005. Inactivating intracellular antiviral responses during adenovirus infection. Oncogene **24:**7686-96.
155. **Wilkinson, D. E., and S. K. Weller.** 2006. Herpes simplex virus type I disrupts the ATR-dependent DNA-damage response during lytic infection. J Cell Sci **119:**2695-703.
156. **Wilkinson, D. E., and S. K. Weller.** 2004. Recruitment of cellular recombination and repair proteins to sites of herpes simplex virus type 1 DNA replication is dependent on the composition of viral proteins within prereplicative sites and correlates with the induction of the DNA damage response. J Virol **78:**4783-96.
157. **Williams, R. S., G. Moncalian, J. S. Williams, Y. Yamada, O. Limbo, D. S. Shin, L. M. Groocock, D. Cahill, C. Hitomi, G. Guenther, D. Moiani, J. P. Carney, P. Russell, and J. A. Tainer.** 2008. Mre11 dimers coordinate DNA end bridging and nuclease processing in double-strand-break repair. Cell **135:**97-109.
158. **Williams, R. S., and J. A. Tainer.** 2005. A nanomachine for making ends meet: MRN is a flexing scaffold for the repair of DNA double-strand breaks. Mol Cell **19:**724-6.
159. **Woo, J. L., and A. J. Berk.** 2007. Adenovirus ubiquitin-protein ligase stimulates viral late mRNA nuclear export. J Virol **81:**575-87.
160. **Xiao, Y., and D. T. Weaver.** 1997. Conditional gene targeted deletion by Cre recombinase demonstrates the requirement for the double-strand break repair Mre11 protein in murine embryonic stem cells. Nucleic Acids Res **25:**2985-91.
161. **Xue, Y., J. S. Johnson, D. A. Ornelles, J. Lieberman, and D. A. Engel.** 2005. Adenovirus protein VII functions throughout early phase and interacts with cellular proteins SET and pp32. J Virol **79:**2474-83.
162. **Yoder, S. S., and S. M. Berget.** 1986. Role of adenovirus type 2 early region 4 in the early-to-late switch during productive infection. J Virol **60:**779-81.
163. **You, Z., J. M. Bailis, S. A. Johnson, S. M. Dilworth, and T. Hunter.** 2007. Rapid activation of ATM on DNA flanking double-strand breaks. Nat Cell Biol **9:**1311-8.
164. **Zhao, S., Y. C. Weng, S. S. Yuan, Y. T. Lin, H. C. Hsu, S. C. Lin, E. Gerbino, M. H. Song, M. Z. Zdzienicka, R. A. Gatti, J. W. Shay, Y. Ziv, Y. Shiloh, and E. Y. Lee.** 2000. Functional link between ataxia-telangiectasia and Nijmegen breakage syndrome gene products. Nature **405:**473-7.
165. **Zhao, X., R. J. Madden-Fuentes, B. X. Lou, J. M. Pipas, J. Gerhardt, C. J. Rigell, and E. Fanning.** 2008. Ataxia telangiectasia-mutated damage-

signaling kinase- and proteasome-dependent destruction of Mre11-Rad50-Nbs1 subunits in Simian virus 40-infected primate cells. J Virol **82:**5316-28.

166. **Zheng, N., B. A. Schulman, L. Song, J. J. Miller, P. D. Jeffrey, P. Wang, C. Chu, D. M. Koepp, S. J. Elledge, M. Pagano, R. C. Conaway, J. W. Conaway, J. W. Harper, and N. P. Pavletich.** 2002. Structure of the Cul1-Rbx1-Skp1-F boxSkp2 SCF ubiquitin ligase complex. Nature **416:**703-9.
167. **Zhong, S., P. Salomoni, and P. P. Pandolfi.** 2000. The transcriptional role of PML and the nuclear body. Nat Cell Biol **2:**E85-90.
168. **Zhu, J., S. Petersen, L. Tessarollo, and A. Nussenzweig.** 2001. Targeted disruption of the Nijmegen breakage syndrome gene NBS1 leads to early embryonic lethality in mice. Curr Biol **11:**105-9.
169. **Zou, L., and S. J. Elledge.** 2003. Sensing DNA damage through ATRIP recognition of RPA-ssDNA complexes. Science **300:**1542-8.

Appendix

Prior to studying the MRN complex in relation to E4-ORF6/E1B-55K, I attempted to create constructs necessary to perform live cell imaging during the early phase of infection following the viral genome. In particular, I was focused on visualizing the association between PML nuclear bodies and the viral genome. An association between the PML nuclear bodies and DNA viral genomes has been observed. In HSV-1, the viral transcriptional regulatory protein, ICP4, binds strongly to viral genomes and is found localized almost exclusively with the viral DNA. This allows for live cell imaging studies with the HSV-1 genome visualized with an ICP4 fusion protein (47). For Ad, *in situ* hybridization has been used to visualize this association (61), but the analogous transcriptional regulatory protein of Ad is the immediate early protein E1A. This protein also functions in regulating transcription of cellular genes and is localized in a diffuse nuclear pattern. Since viral protein VII is found associated with the viral genome during the initial phase of infection, this suggests that by making a pVII fusion protein, visualization of the viral genome can occur in the context of a live cell early during an infection while the initial association of the genome with the PML bodies is taking place.

Specific Aim. Create a live cell imaging system to study PML Bodies and the establishment of replication domains

Many DNA viruses (e.g. HSV, CMV, Adenovirus) target PML bodies (also referred to as PML Oncogenic Domains (PODs) or ND10s) as nuclear sites where the establishment of replication domains can occur. Whether this association is conferred by the host cell as an innate immune response to the virus, or by the virus as a means to efficiently replicate, has yet to be determined. I plan to create a system to perform live cell imaging of Adenovirus-infected cells and visualize the viral genome, POD-associated proteins, and viral proteins to gain further understanding of the correlation between PML bodies and DNA virus establishment of replication domains. I also intend on using $PML^{-/-}$ MEFs to explore viral deposition in the absence of PML bodies.

Visualization of PML bodies in live cells

Fusions of proteins associated with the PML bodies are required to visualize these subnuclear structures in live cells. Two expression vectors, CFP-PML I and EYFP-Sp100 were obtained from the Dr. David Spector lab and an EYFP-PML I fusion was created in the lab by swapping the CFP gene with the EYFP gene. Also, an EYFP-Sp100-expressing U2OS cell line was obtained from Maria Chen of the Dr. David Spector lab. E4ORF3 was able to rearrange these fusion proteins during an infection (Fig. A1 A-C).

Construction of an ECFP-ORF3 virus

An ECFP-ORF3 fusion was created and cloned into the viral genome in place of the wild type ORF3 gene with the intent of using the virus in live

cell imaging experiments. Both N-terminal and C-terminal fusions were made, however, the C-terminal fusion, ORF3-ECFP, was not able to rearrange PML bodies in a normal time frame. The N-terminal fusion, ECFP-ORF3, was able to rearrange PML bodies, however, filamentous cytoplasmic accumulations form as well (Fig. A1 D-F). The ECFP-ORF3 fusion was introduced into a virus that lacks ORF6 expression (dl355) and replaced the ORF3 gene. Expression and localization was visualized by immunofluorescence and found to be similar to the former virus (Fig. A2). dl355/ECFP-ORF3 was able to complement for growth, demonstrating the functionality of the fusion protein, and infect with a PFU ratio of 35:1, while wild type is 20:1.

Construction of a pVII-EYFP virus

The N-terminus of the pVII protein becomes proteolytically cleaved off to form the mature VII protein late during Ad assembly. This restricts the location of the EYFP fusion to the C-terminus of the protein. Initially, construction of a virus that contained only the pVII-EYFP fusion in its natural position in the L2 region and not the wild type pVII protein was attempted. The initial plan involved subcloning the Ad5 fragment from nt 10,609 (XbaI) to nt 19,718 (BsrGI) from pTG3602 into the pBS polylinker. The NheI site at nt 10,808 needed to be removed so an NheI site could be created to disrupt the TAG stop codon of pVII and be used to clone in the EYFP gene. This was performed by fusing it with the cohesive end of the XbaI site at nt 10, 609. Quick-change mutagenesis was attempted to alter the TAG stop codon to an NheI site, however, this did not work for an unknown reason and a fusion PCR method was used instead as shown in Figure A3. The first step involves using PCR to create two fragments with overlapping sequences at the stop codon of pVII. The primers were constructed such that the stop codon was absent and in its place an NheI site was created. A second round of PCR was performed combining the two PCR products from the first step and using the primers at the far left and far right to create one large PCR product. These primers included an AscI site at the left and NdeI site at the right so that it could be ligated back into the pBS-pVII plasmid.

The EYFP gene was amplified by PCR with an NheI site at the 5' end that would lead to an in-frame ligation product with the pVII gene. The ligation did not work either so another fusion PCR method was used. In this instance, PCR was used to create three fragments with overlapping sequences created by primers with excess sequence that is complementary to another piece of DNA as shown in Figure A4. The 521 bp of sequence upstream of the pVII gene in the plasmid pBS-pVII-NheI was amplified with a primer that added on several bp of the 5' sequence of the EYFP gene to the 3' end. The EYFP was then amplified with pVII sequence at its 5' end and downstream Ad sequence at its 3' end. Finally, the 409 bp fragment of Ad sequence downstream of the pVII gene in the pBS-pVII-NheI plasmid was amplified with sequence from the 3' end of EYFP added onto the 5' end of the Ad fragment. The second step involves combining the pVII and EYFP

fragments in a PCR reaction with primers to the 5' end of the pVII fragment and the 3' end of the EYFP fragment. Next, fusion of the three fragments is completed by combining the pVII-EYFP fragment with the fragment containing the downstream Ad sequences with left and right primers in a PCR reaction. Finally, homologous recombination can be used to insert this large PCR product into the pBS-pVII-NheI plasmid that has been digested with NheI.

Finally, recombination of the pVII-EYFP gene product with pTG3602 was performed. pTG3602 was digested with FseI and the fragment with the backbone was purified. This fragment was missing the region from nt 12,612 to nt 17,774, but had overlapping regions with the pVII portion of Ad5 originally cloned into pBS (nt 10,609 to nt 19,718). Unfortunately, however, this virus was unable to grow in cell culture. There were several possible reasons for this inability to grow. One is the possibility that at some point during the cloning process, a detrimental mutation occurred. To rule this out, the entire 4kb region that had been amplified by PCR was sequenced and found to be correct. A second possibility is that the insertion of the EYFP sequence prevented the correct splicing of the pV gene. The start codon of pV lies about 50 bp downstream of the pVII stop codon, however, the putative branch site appears to be intact. A third reason could be the functional disruption of the pVII protein either by the inability to bind DNA and reorganize the genomic structure to allow for transcription and replication or by interfering with packaging due to a size constraint (i.e. the greater than 1,000 copies of pVII-EYFP that coat the viral DNA may be too large with the EYFP addition to fit inside the capsid). If the problem were due to pV disruption or packaging interference, a virus that contains a separate pVII-EYFP gene would correct for these and grow. The fluorescence intensity would be lower due to the presence of the wild type pVII protein, however, since about 1,080 molecules are thought to coat the DNA, visualization should still be possible. Construction of a virus that lacks expression of the E1 genes and instead expresses pVII-EYFP under the control of the major late promoter (MLP) and downstream of the tripartite leader (TPL), as it is organized in the wild type virus, became the next approach employed. When infected into cells that express the E1 genes or co-infected with a helper virus, virions with VII-EYFP-coated DNA will be produced.

Construction of an E1-replacement pVII-EYFP virus

The pNL3C plasmid is a left end Ad E1-expression vector that contains the MLP-TPL. Primers were created to add BamHI sites to the ends of pVII-EYFP so that it could be ligated into pNL3C. Again, there was difficulty with this cloning process and another fusion PCR method was employed as shown in Figure A5. In this instance, the 850 bp of sequence upstream of the TPL in the plasmid pNL3C was amplified with a primer that added on the several bp of the 5' sequence of the pVII gene. The pVII-EYFP gene that had been cloned was then amplified with TPL sequence at its 5' end and downstream Ad sequence at its 3' end. Finally, the 1820 bp fragment of Ad sequence downstream of the TPL in the pNL3C plasmid was amplified with

sequence from the 3' end of EYFP added onto the 5' end of the Ad fragment. The second step involves combining the TPL and pVII-EYFP fragments in a PCR reaction with primers to the 5' end of the TPL fragment and the 3' end of the pVII-EYFP fragment. Next, fusion of the three fragments is completed by combining the TPL-pVII-EYFP fragment with the fragment containing the downstream Ad sequences with left and right primers in a PCR reaction. Finally, homologous recombination can be used to insert this large PCR product into the pNL3C plasmid that has been cut in the center of the replaced region with SalI.

The resulting pNL3C-pVII-EYFP plasmid was linearized with EcoRI and transfected into N52-cre cells, which express E1 proteins, along with the right end of ClaI-cut ΔE4 1-3 viral DNA. Virus was grown up and used to infect A549 cells. Unfortunately, there was only weak fluorescence after translocation into the nucleus and this virus could not be used to infect cells for live cell imaging. The level of VII-EYFP packaged versus wild type VII (Fig. A6 A), as well as the amount of pVII-EYFP produced within the infected cells (Fig. A6 B), was evaluated by Western blot. Around the same amount of protein was produced in the cells, however, only a small portion of the fusion protein was being packaged as compared to wild type VII. Another virus was then created that had further deletions in the E1B and E3 regions to create more space within the capsid to allow for more VII-EYFP molecules to be packaged. The E1B deletion was made by digesting the pNL3C-pVII-EYFP plasmid with HpaI and BglII, isolating the large fragment, creating blunt ends with Klenow, and ligating the plasmid together. The E3 deletion was created temporarily by recombining with dl7001. This virus would then contain E4-ORF3, which would be unfavorable for experiments that look to study the affects E4-ORF3. If this virus allowed for visualization of the viral genome during live cell imaging, a virus that also lacks E4-ORF3 could then be constructed. The EYFP signal from this virus appeared to become less intense after 2-3 hpi. It occurred to me that the fluorescent protein may be destroyed during acidification of the endosome during the initial phase of infection.

Construction of acid-resistant pVII-fusion viruses

Plasmids expressing acid-resistant fluorescent proteins, SCFP-2 and TagRFP, were obtained from Dr. Samuel Campos. These genes were substituted into the pNL3C-ΔE1B-VII-EYFP plasmid in place of EYFP using another fusion PCR method. The new plasmids were recombined with dl327 (a different E3-deleted virus) and ΔE4 1-3. The ΔE4 1-3/SCFP virus appeared to have a small amount of VII-SCFP encapsidated in the virions (Fig. A6 C). Unfortunately, none of the virions produced visualizable viral genomes within infected cells and the project was abandoned.

Figure A1.

Expression and localization of EYFP-Sp100 and ECFP-ORF3. U2OS-EYFP-Sp100 cells were infected with E4ORF6$^-$ at 200p/cell (A-C) or the ECFP-ORF3 virus (D-F) for 18 hrs. and immunostained for E4ORF3 using the 6A11 antibody with a TRITC-labeled secondary antibody (B). Images were taken with a YFP filter (A, D) and a CFP filter (E). Merged images (C, F) show colocalization.

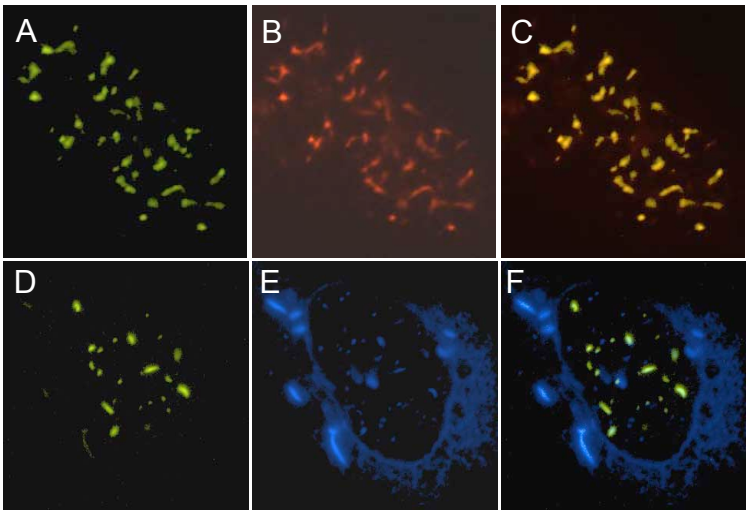

Figure A2.

Expression and localization of dl355/ECFP-ORF3. Immunofluorscence microscopy of dl355/ECFP-ORF3 virus-infected A549 cells fixed at 6 (A-D) or 16 (E-H) hpi and immunostained with an αDBP antibody (B, F). Images were taken using DIC (differential interference contrast) microscopy (A, E) or fluorescence microscopy with the TRITC (B, F) or CFP filter (C, G).

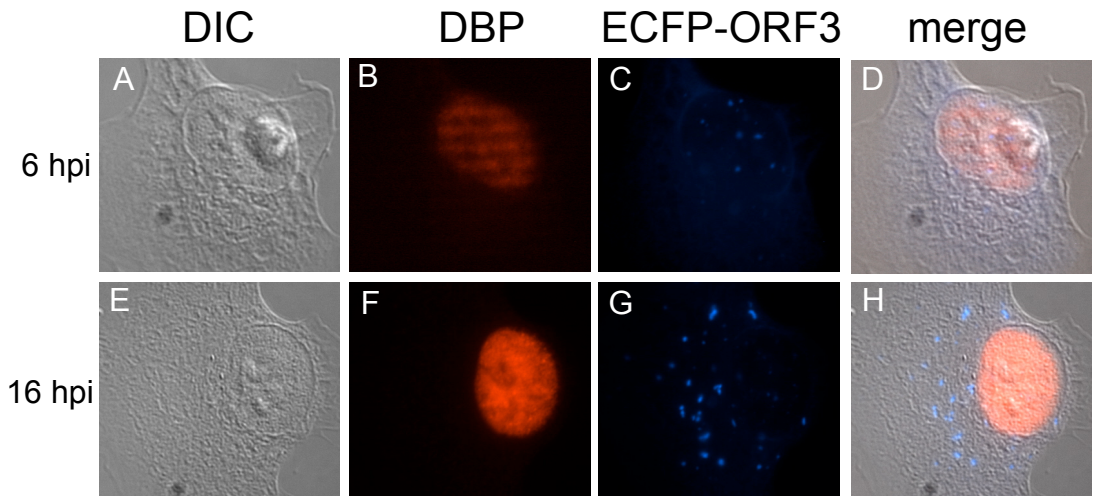

Figure A3.

Fusion PCR schematic to create NheI site in place of TAG stop codon in pVII gene.

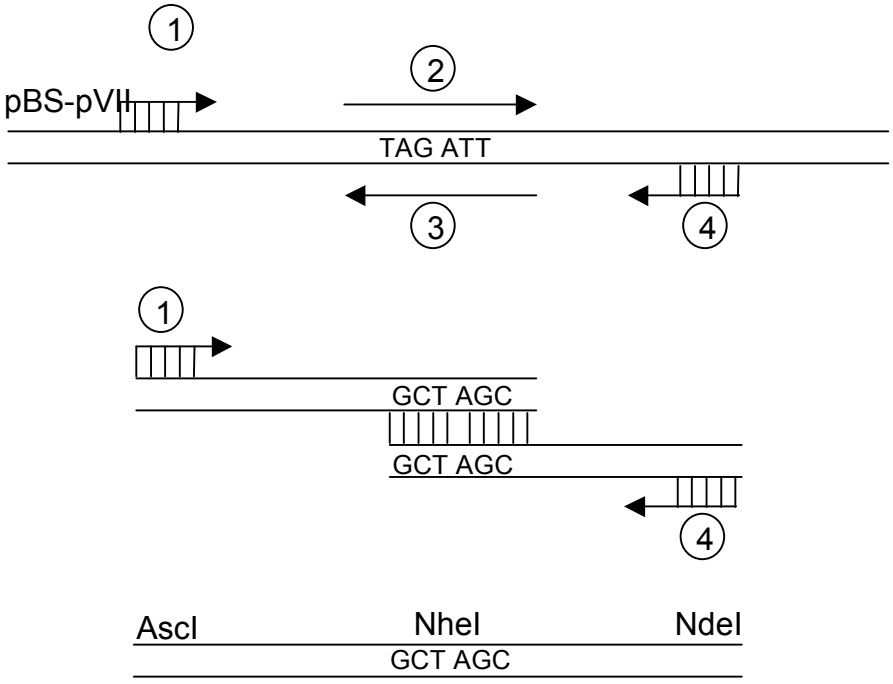

1. Ad 15658-15673 5'- GAA CCA GAT TTT GGC G -3'
2. pVII-TGA-1 5'- CCC CGC GCA ACG CTA GCG CAA GAA AAA ACT A -3'
3. pVII-TGA-2 5'- TAG TTT TTT CTT GCG CTA GCG TTG CGC GGG G -3'
4. Ad 19563-19548 5'- GTG GGT TTT GCA TAT G -3'

Figure A4.

Fusion PCR schematic to create a pVII-EYFP fusion.

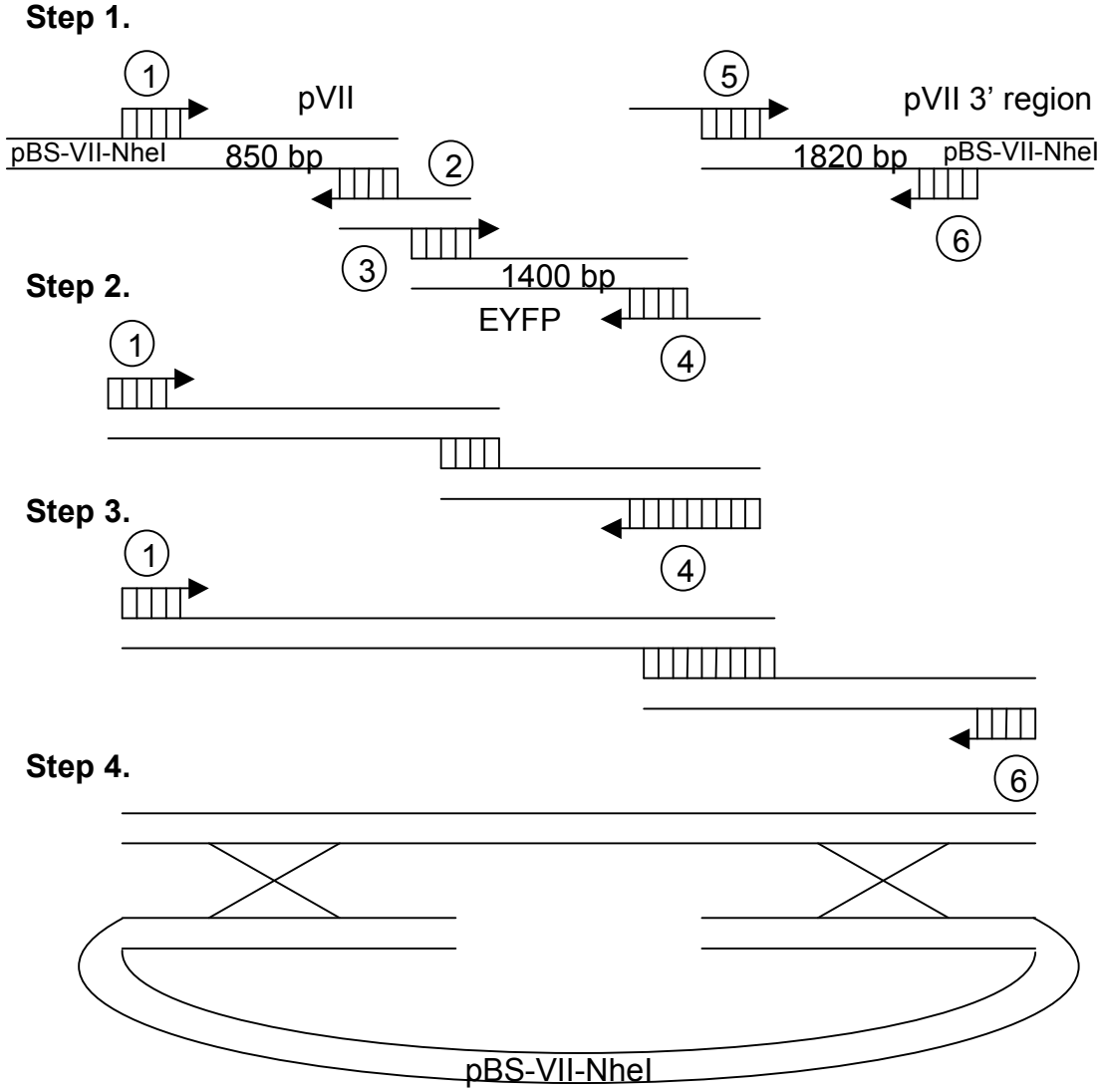

1	Ad 15950-15965	5'- GCC AAG AAG CGC TCC -3'
2	KK-2	5'- GTG GCG ACG CTA GCG TTG CGC -3'
3	KK-3	5'- CAA CGC TAG CGT CGC CAC CAT GGT G -3'
4	KK-4	5'- GTT TTT TCT TGC TTA CTT GTA CAG CTC GT -3'
5	KK-5	5'- GTA CAA GTA AGC AAG AAA AAA CTA CTT AG -3'
6	Ad 16887-16873	5'- CCG AGG CGC TCG TTG -3'

Figure A5.

Fusion PCR schematic to insert the pVII-EYFP fusion gene in an E1-replacement plasmid.

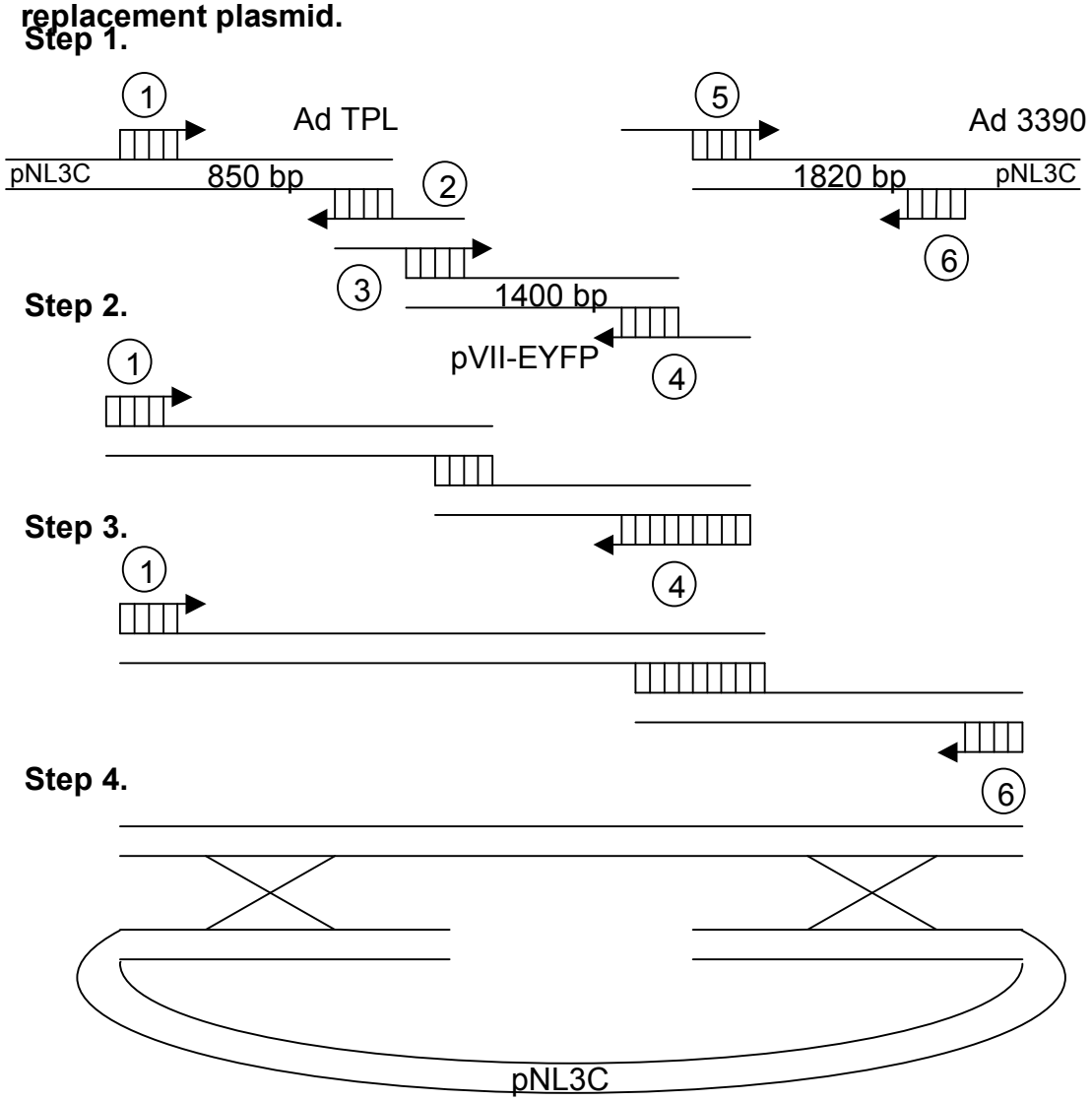

1	Ad 1-27	5'- CAT CAT CAA TAA TAT ACC TTA TTT TGG -3'
2	pVII-YFP-TPL-2	5'- GAC ATG GTC TTG CGA CTG TGA C -3'
3	pVII-YFP-5-2	5'- TCG CAA GAC CAT GTC CAT CCT TAT AC -3'
4	pVII-YFP-3-2	5'- CGT TAA CCA TTA CTT GTA CAG CTC GTC -3'
5	pVII-YFP-1570-2	5'- TAC AAG TAA TGG TTA ACG CCT TTG -3'
6	E1B-17	5'- GCC ACA CTC GCA GGG TC -3'

Figure A6.

Biochemical analyses of VII fusion proteins. VII fusion proteins were evaluated by 15% SDS-PAGE followed by immunoblotting with an αVII antibody. (A) Purified virions of dl309 and VII-EYFP (1.2 x 10^{12} particles). (B) RIPA lysates from dl309 or VII-EYFP-infected 293 cells. (C) Purified virions of dl309, dl327/SCFP, ΔE41-3/SCFP, or ΔE41-3/TagRFP.